

621.385.6

ELECTRON-BEAM TRANSVERSE-WAVE PARAMETRIC AMPLIFIERS

V. M. LOPUKHIN and A. S. ROSHAL'

Usp. Fiz. Nauk 85, 297-334 (February, 1965)

CONTENTS

Introduction	
1. Method of Coupled Modes	117
2. Transverse Waves of Electron Beam	120
3. Mechanism of Parametric Amplification	122
4. Input (Output) Device for Coupling with a Fast Cyclotron Wave	127
5. Sources of Amplifier Noise	130
6. Generalization of the Principle of Parametric Amplification	132
7. Types of Amplifiers	134
Conclusion	137
Cited Literature	138

INTRODUCTION

THE principles of parametric amplification of waves in an electron beam are presently under extensive discussion in the scientific literature. Electron-beam parametric amplifiers, which represent a promising trend in the field of electron beam amplifiers for microwave frequencies^[1-5], are based on these principles. Application of parametric action to the electron beam makes it possible to amplify the so-called fast waves of the electron beam, making feasible in many cases amplifiers with many advantages over other microwave amplifiers. The advantages of electron beam parametric amplifiers are, for example, high amplification stability, directivity (that is, absence of external feedback through the beam and the slow-wave system), good phase stability, lack of dependence of bandwidth on gain, ability to withstand large microwave overloads, and of particular importance, the possibility of obtaining a noise figure close to that of quantum amplifiers or parametric semiconductor amplifiers^[2].

An extensive literature has been devoted to electron beam parametric amplifiers. Principal attention will be paid in this paper to the physical principles of parametric amplification of transverse waves of an electron beam, with a consideration of the most interesting among the pertinent problems. Such problems, for example, are the mechanism of amplification, the sources of amplifier noise, the noise-removal mechanism and band in the input devices, ways of reducing the noise figure of amplifiers and of increasing the gain bandwidth (noise elimination), effect of the scatter of longitudinal velocity and of space charge, problems of coupling between different modes at the signal and pump frequencies, the transfer of noise from various waves into the signal wave,

etc. The construction of various amplifiers will be briefly described.

Parametric amplifiers for electron-beam transverse waves can be broken up into two classes: amplifiers with alternating electric field in the amplification region, and amplifiers with electrostatic field. We consider both classes, and for brevity denote the amplifiers with variable field as EPA (electron-beam parametric amplifiers), and those with electrostatic field ESA (electrostatic amplifiers).^{*} There are also amplifiers with alternating or constant magnetic field in the amplification region. Therefore the designation EPA will sometimes include all amplifier modifications.

1. METHOD OF COUPLED MODES

We consider an electron beam with modulation of the transverse velocities and coordinates at a frequency ω , moving with constant velocity u_0 in a constant magnetic field $\mathbf{B}\{0, 0, B_0\}$ and an alternating electric field $\mathbf{E}\{E_x, E_y, 0\}$. We assume that the beam is infinitesimally thin and there is no space-charge field. The motion of the individual electron then coincides with the motion of the beam as a whole, and is described by the usual system of equations

$$m \frac{d\mathbf{v}}{dt} = -|e|\mathbf{E} + [\mathbf{v}\mathbf{B}], \quad \frac{d\mathbf{r}}{dt} = \mathbf{v}. \quad (1.1)^\dagger$$

If the beam is of constant cross section, Eqs. (1.1) correspond to the motion of the center of mass of the beam cross section.

^{*}It must be noted that these designations are not universally accepted. Many authors do consider electrostatic amplifiers to be parametric.

[†] $[\mathbf{v}\mathbf{B}] = \mathbf{v} \times \mathbf{B}$.

Assuming that all the variables are proportional to $\exp(i\omega t)$, with*

$$\frac{d}{dt} = \frac{\partial}{\partial t} + \frac{\partial}{\partial z} \frac{dz}{dt} = i\omega + u_0 \frac{\partial}{\partial z}, \quad (1.2)$$

we obtain a system of equations for the amplitude of the transverse velocities and displacements

$$\frac{\partial v_x}{\partial z} = -i\beta_e v_x - \beta_c v_y - \frac{\eta}{u_0} E_x, \quad (1.3)$$

$$\frac{\partial v_y}{\partial z} = -i\beta_e v_y + \beta_c v_x - \frac{\eta}{u_0} E_y, \quad (1.4)$$

$$\frac{\partial x}{\partial z} = -i\beta_e x + \frac{v_x}{u_0}, \quad (1.5)$$

$$\frac{\partial y}{\partial z} = -i\beta_e y + \frac{v_y}{u_0}, \quad (1.6)$$

where

$$\eta = \frac{|e|}{m}, \quad \beta_e = \frac{\omega}{u_0}, \quad \beta_c = \frac{\omega_c}{u_0}, \quad \omega_c = \eta B_0, \quad (1.7)$$

and ω_c is the cyclotron frequency. In (1.3) we can write d/dz in place of $\partial/\partial z$, since the amplitude depends on no other arguments.

The system (1.3)–(1.6) is inconvenient because each equation contains several variables, for example (1.3) contains v_x and v_y , etc. There is a possibility of separating the variables. Let us multiply, for example, (1.4) by i and let us add it to (1.3); this yields

$$\frac{\partial v_+}{\partial z} = -i(\beta_e - \beta_c)v_+ - \frac{\eta}{u_0} E_+, \quad v_+ \equiv v_x + iv_y, \quad E_+ \equiv E_x + iE_y, \quad (1.8)$$

where v_+ is a new variable. Multiplying (1.4) by i and subtracting it from (1.3), we get

$$\frac{\partial v_-}{\partial z} = -i(\beta_e + \beta_c)v_- - \frac{\eta}{u_0} E_-, \quad v_- \equiv v_x - iv_y, \quad E_- \equiv E_x - iE_y. \quad (1.9)$$

We proceed analogously with (1.5) and (1.6); taking account of (1.8) and (1.9), we obtain finally the following system of equations of motion:

$$\left. \begin{aligned} \frac{\partial a_1}{\partial z} &= -i\beta_1 a_1 - \eta \frac{\gamma}{u_0} E_+, & \beta_1 &= \beta_e - \beta_c, \\ \frac{\partial a_2}{\partial z} &= -i\beta_2 a_2 - \eta \frac{\gamma}{u_0} E_-, & \beta_2 &= \beta_e + \beta_c, \\ \frac{\partial a_3}{\partial z} &= -i\beta_3 a_3 - \eta \frac{\gamma}{u_0} E_+, & \beta_3 &= \beta_e, \\ \frac{\partial a_4}{\partial z} &= -i\beta_4 a_4 - \eta \frac{\gamma}{u_0} E_-, & \beta_4 &= \beta_e, \end{aligned} \right\} \quad (1.10)$$

where

$$\gamma = \left(\frac{|I_0|}{8\eta} \right)^{1/2}, \quad (1.11)$$

$$a_1 = \gamma v_+, \quad a_2 = \gamma v_-, \quad (1.12)$$

$$a_3 = a_1 - i\omega_c \gamma r_+, \quad a_4 = a_2 + i\omega_c \gamma r_-, \quad r_{\pm} = x \pm iy, \quad (1.13)$$

I_0 is the dc current of the beam and γ is a normalization factor.

The new variables a_1, \dots, a_4 are called the proper transverse waves of the electron beam; the physical

picture will be considered in Sec. 2. The transition from the system (1.3)–(1.6) to (1.10) is called transformation to the proper waves of the electron beam. The normalization coefficient γ is chosen such that the power P_j carried by the wave a_j is conveniently expressed in terms of its amplitude. It is known that the power of transverse waves of an electron beam is proportional to their frequency ω ^[6-8]; taking this into account, the factor γ (1.11) is taken such that

$$P_j = \frac{\omega}{\omega_c} |a_j|^2. \quad (1.14)$$

We see from (1.10) that the waves a_1, \dots, a_4 are not coupled in the drift region, where $\mathbf{E} = 0$. The electric field \mathbf{E} couples the waves, and the character of this coupling is determined by the form of the field \mathbf{E} .

The group of procedures which we have applied here to a particular example is developed in the general coupled-mode method. The method of coupled modes has been extensively in use, ever since the papers of J. Pierce^[9,10], because of its effectiveness and physical clarity. The most complete and exhaustive explanation of the method, with applications to the theory of microwave devices, is contained in the book of W. Louisell^[11]. M. Pease^[12-17] developed in his mathematically rigorous papers a generalized schematized theory of linear converters (input coupling devices, amplifiers, etc.), while the concept of coupled modes is based on matrix theory.

The method of coupled modes, as applied to the problem considered here, can be briefly described as follows. Assume that we have a physical system which is uniformly distributed along the coordinate z . This may be, for example, a transmission line (isolated or coupled, possibly with parametric action), electron beams (possibly coupled with transmission lines), etc. Propagating along the system is a finite (or even infinite) number of waves, for each of which we can write a linear differential equation. For example, the system (1.3)–(1.6) describes propagation of transverse velocity and displacement waves; voltage, current, variable electron-beam charge density, and other waves are also possible. The physical system is thus characterized by a so-called coupled-mode vector \mathbf{w} , which is an aggregate of all the waves of the system; in our example

$$\mathbf{w} = \begin{pmatrix} v_x \\ v_y \\ x \\ y \end{pmatrix}. \quad (1.15)$$

The differential equations are best written in matrix form^[18]:

$$\frac{\partial \mathbf{w}}{\partial z} = \dot{-} iR_1 \mathbf{w} - \mathbf{e}_1, \quad (1.16)$$

where R_1 is the matrix of the equation and \mathbf{e}_1 is the vector of the electric field intensity. The components of the vector \mathbf{w} form the basis of the system (1.16).

*The quantities $\frac{dx}{dt}$ and $\frac{dy}{dt}$ are assumed small and are omitted when taking the derivative d/dt .

For example, for (1.3)–(1.6),

$$R_1 = \begin{pmatrix} \beta_e & -i\beta_c & 0 & 0 \\ i\beta_c & \beta_e & 0 & 0 \\ \frac{i}{u_0} & 0 & \beta_e & 0 \\ 0 & \frac{i}{u_0} & 0 & \beta_e \end{pmatrix}, \quad \mathbf{e}_1 = \frac{\eta}{u_0} \begin{pmatrix} E_x \\ E_y \\ 0 \\ 0 \end{pmatrix}. \quad (1.17)$$

We shall assume that the matrix R_1 can be reduced to diagonal form R by a similarity transformation with the aid of the matrix T :

$$R = TR_1T^{-1} \quad (1.18)$$

(R is a diagonal matrix and the determinant $|T| \neq 0$). Such a possibility usually exists in cases of physical interest^[13,16].

We now introduce new variables \mathbf{a} , linearly connected with the old ones:

$$\mathbf{a} = T\mathbf{w}, \quad (1.19)$$

that is, we change the basis. Multiplying (1.16) from the left by the matrix T and using the inverse transformation

$$\mathbf{w} = T^{-1}\mathbf{a}, \quad (1.20)$$

we obtain an equation

$$\frac{d\mathbf{a}}{dz} = -iR\mathbf{a} - \mathbf{e}_0 \quad (\mathbf{e}_0 = T\mathbf{e}_1) \quad (1.21)$$

with a diagonal matrix R . The change of the basis (1.19) is called transformation to the natural modes of the system \mathbf{a} ; from the mathematical point of view it represents a transition to a basis made up of the eigenvectors of the matrix^[19]. Thus, in the case under consideration of (1.10)–(1.13),

$$\mathbf{a} = \begin{pmatrix} a_1 \\ a_2 \\ a_3 \\ a_4 \end{pmatrix}, \quad R = \begin{pmatrix} \beta_1 & 0 & 0 & 0 \\ 0 & \beta_2 & 0 & 0 \\ 0 & 0 & \beta_3 & 0 \\ 0 & 0 & 0 & \beta_4 \end{pmatrix}, \quad \mathbf{e}_0 = \frac{\sqrt{G_0}}{4} \begin{pmatrix} E_+ \\ E_- \\ E_+ \\ E_- \end{pmatrix}, \quad (1.22)$$

and

$$T = \gamma \begin{pmatrix} 1 & i & 0 & 0 \\ 1 & -i & 0 & 0 \\ 1 & i & -i\omega_c & \omega_c \\ 1 & -i & i\omega_c & \omega_c \end{pmatrix},$$

$$T^{-1} = \frac{1}{2\gamma} \begin{pmatrix} 1 & 1 & 0 & 0 \\ -i & i & 0 & 0 \\ -\frac{i}{\omega_c} & \frac{i}{\omega_c} & \frac{i}{\omega_c} & -\frac{i}{\omega_c} \\ -\frac{1}{\omega_c} & -\frac{1}{\omega_c} & \frac{1}{\omega_c} & \frac{1}{\omega_c} \end{pmatrix}, \quad (1.23)$$

where $G_0 = |I_0|/U_0$ is the dc conductance of the beam. In the drift space ($\mathbf{e}_0 = 0$), the modes a_j are not coupled, since the matrix R is diagonal; when $\mathbf{e}_0 \neq 0$ the modes are coupled because of the electric field. Thus, a parametric amplifier contains a pump generator, which produces a pumping wave whose field couples the different modes and ensures amplification.

Usually the field \mathbf{e}_0 can be represented by a linear combination of coupled modes a_j (sometimes it is necessary to introduce for this purpose additional waves, for example, the transmission-line wave producing this field). The equation of the coupled waves is then written in the form of a homogeneous differential equation

$$\frac{d\mathbf{a}}{dz} = -iR\mathbf{a}, \quad (1.24)$$

where the matrix is

$$R = \begin{pmatrix} \beta_1 & c_{12} & c_{13} & \dots & c_{1m} \\ c_{21} & \beta_2 & c_{23} & \dots & c_{2m} \\ c_{31} & c_{32} & \beta_3 & \dots & c_{3m} \\ \dots & \dots & \dots & \dots & \dots \\ c_{m1} & c_{m2} & c_{m3} & \dots & \beta_m \end{pmatrix}. \quad (1.25)$$

The off-diagonal elements c_{jk} are called the coupling coefficients; if the coefficients $c_{jk} \neq 0$, then coupling exists between waves j and k . If the matrix R is of high order, the solution of the system of differential equations entails great difficulties. Special methods are being developed in the theory of coupled modes for the analysis and solution of equations of the type (1.24) (see, in particular, the papers of M. Pease^[12,14,16]). The main criterion in such an analysis is the extent of coupling between the individual modes.

A distinction is made between weak and strong mode couplings. Louisell^[11] recommends that the degree of coupling between two modes j and k be defined in terms of the coefficient

$$F = \left[1 - \left(\frac{\beta_j - \beta_k}{2} \right)^2 \frac{1}{c_{jk}c_{kj}} \right]^{-1}, \quad (1.26)$$

where β_j , β_k , c_{jk} , and c_{kj} are elements of the matrix (1.25). Coupling is regarded as weak if $F \ll 1$ and strong if F is of the order of unity.* An interchange of energy takes place between strongly coupled modes, leading to a mutual amplification (active coupling) or to a periodic energy exchange (passive coupling). The most important is the active coupling between any two waves, which is of principal importance for amplifier operation. However, in addition to this, a few other modes are passively coupled with each mode. These couplings do not lead to amplification and are sources of additional loss and noise. Interference between different modes is also possible.

The waves in an electron beam are characterized by their kinetic power, by which is meant the high-frequency energy carried by the given wave through a section of the beam per unit time. This high-frequency energy constitutes the difference between the average kinetic energy of the electrons in the beam excited at the given wavelength and the average kinetic

*A criterion for strong coupling, as applied to parametric amplifiers, is given in Sec. 3.

energy of the unexcited beam. According to this definition, the kinetic power can be either positive or negative. Accordingly, the modes excited in an electron beam can be either fast or slow.

When a fast mode is excited in the beam the kinetic power, i.e., the kinetic energy carried by the beam electrons per unit time, becomes larger on the average than the kinetic power of the unperturbed beam. This is connected with the fact that upon excitation of a fast mode the electrons become accelerated, that is, their average longitudinal velocity increases (this is why the mode is called fast). Thus, the kinetic power of a fast mode is positive. When a slow mode is excited in the beam, the electrons are decelerated, and the kinetic power of the beam decreases in the mean compared with the kinetic power of the unperturbed beam. Consequently, the kinetic power of a slow mode is negative.

In a decelerating system coupled to the beam, two waves can propagate—forward and backward. The flux of high-frequency power is positive in the forward wave and negative in the backward wave. The electron beam can also contain fast and slow space-charge waves, and also fast and slow transverse waves (cyclotron and synchronous, Sec. 2).

If the eigenvalues of the matrix R (1.25) satisfy certain definite relations^[14,15], then conservation laws hold in such a system. Namely: there exist quadratic forms such as

$$q(Q) = \mathbf{a}^+ Q \mathbf{a}, \quad (1.27)$$

where Q are certain matrices, called metrics and determined by the type of the system; these forms are invariant, that is, $dq/dz = 0$.^{*} One such quadratic form is the high-frequency power of the system, which is the sum of the powers carried by the different modes each taken with the proper sign. The invariance of the power is known in the theory of electron-beam devices as the kinetic-power theorem^[20-23] and is the consequence of the law of conservation of the energy propagating in the beam and in the line coupled with it (the latter is assumed lossless).

When an electron beam interacts with a passive device (slow-wave system, resonator), the electrons give up part of their energy to the device and, in the mean, are slowed down. The kinetic power of the beam decreases. It is obviously possible to eliminate with the aid of such passive devices from the beam the fast mode, which carries positive kinetic power, and in particular the fast noise mode. The slow noise mode, the kinetic power of which is negative, cannot be removed from the beam with any passive system. To the contrary, owing to the slowing down of the electron beam, the slow mode may become amplified. This mechanism of amplification is used in ordinary

(non-parametric) microwave amplifiers (traveling-wave tube, electron-wave tube, klystron) that operate with slow waves of the beam. The presence of noise in a slow mode deteriorates the noise factor of such amplifiers.*

Since a passive system cannot serve as a source of energy to increase the positive kinetic power of the fast mode, the latter can be amplified in such amplifiers only if an actively-coupled slow mode is simultaneously amplified. In this case the total power of both amplified waves remains constant, in accordance with the kinetic-power theorem. This amplification mechanism is used, for example, in electrostatic parametric amplifiers. The presence of strong coupling with a slow mode also increases their noise figure, owing to the transfer of noise from the slow mode. However, fast modes, whose noise can be eliminated beforehand can be successfully amplified in parametric amplifiers. The power necessary for the amplification is then supplied by the pump generator.

2. TRANSVERSE WAVES IN AN ELECTRON BEAM

The components a_1 and a_2 of the natural-mode vector \mathbf{a} are called respectively the slow and fast cyclotron waves, while a_3 and a_4 are the synchronous waves. The kinematics of motion of electrons in the different waves was investigated in detail in^[11,24].

In cyclotron waves the separate electrons, and hence the beam as a whole, move along the z axis with velocity u_0 and simultaneously rotate about this axis counterclockwise (we shall be viewing henceforth from the end of the z axis) with angular frequency ω_c . The electrons in these waves have both transverse velocities and transverse displacements. The electrons (and the beam) in the synchronous waves have no transverse velocity and have only longitudinal velocity u_0 and transverse displacement. The noise of the synchronous waves constitutes fluctuations of the center of inertia of the beam cross section. Each wave corresponds to a definite beam configuration.

The beam excited by the fast cyclotron wave has the form of a helix (Fig. 1a) with pitch

$$p_1 = -\frac{2\pi u_0}{\omega - \omega_c}. \quad (2.1)$$

The helix winds in a clockwise direction (pitch $p_1 < 0$) when $\omega > \omega_c$ and counterclockwise ($p_1 > 0$) when $\omega < \omega_c$. As $\omega \rightarrow \omega_c$ we have $p_1 \rightarrow \infty$ and the helix becomes a straight line on which all the electrons are located. The phase velocity of the wave is

$$v_{ph1} = \frac{\omega}{\beta_1} = \frac{u_0}{1 - \frac{\omega_c}{\omega}}. \quad (2.2)$$

When $\omega > \omega_c$ the wave is forward, with $v_{ph1} > 0$, and when

*The method for investigating systems with the aid of their quadratic invariants was developed by M. Pease^[14-16].

*Several special procedures can be used to reduce the noise of slow modes (Secs. 5 and 7).

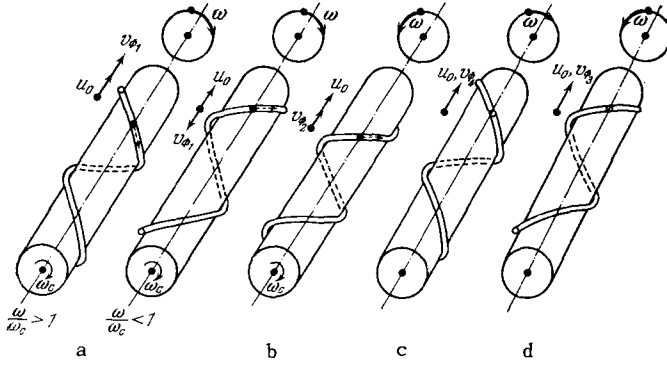


FIG. 1. Transverse waves of electron beam. The inside cylinder is drawn for clarity.

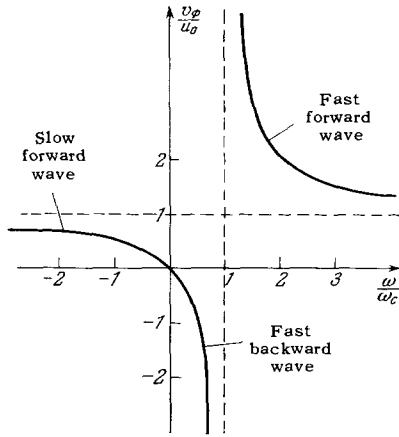


FIG. 2. Dispersion characteristic of cyclotron waves.

$\omega < \omega_c$ it is backward, with $v_{ph1} < 0$. As $\omega \rightarrow \omega_c$ we get $v_{ph1} \rightarrow \infty$ (Fig. 2).

The beam excited by the slow cyclotron wave has the form of a helix (Fig. 1b) with pitch

$$p_2 = \frac{2\pi u_0}{\omega + \omega_c}; \quad (2.3)$$

and the phase velocity of the wave is

$$v_{ph2} = \frac{\omega}{\beta_2} = \frac{u_0}{1 + \frac{\omega_c}{\omega}} < u_0. \quad (2.4)$$

We note that if we admit (mathematically) values $\omega < 0$, then all the equations for the fast waves can be used to describe the slow waves, by going over to the complex-conjugate equation and replacing ω by $(-\omega)$:

$$a_1(-\omega) = a_2^*(\omega), \quad a_3(-\omega) = a_4^*(\omega). \quad (2.5)$$

We shall assume from now on positive and negative values for the frequencies, assuming the fast and slow waves to have positive and frequency, respectively.

Figure 3 shows an ω - β diagram for cyclotron waves. The upper half-plane ($\omega > 0$) corresponds to the fast waves, and the lower one ($\omega < 0$) to the slow waves. The right half-plane ($\beta > 0$) corre-

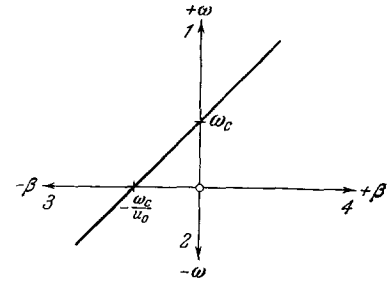


FIG. 3. ω - β diagram of cyclotron waves. 1 - Fast cyclotron wave; 2 - slow cyclotron wave; 3 - right-hand helix; 4 - left-hand helix.

sponds to waves in the form of a left-hand screw, and the left half-plane ($\beta < 0$) to a right-hand screw. The phase velocity is $v_{ph} = \omega/\beta$; for the slow wave it is always positive and for the fast wave it can be either positive or negative.

The beam excited at the synchronous wave a_3 (or a_4) has a helix pitch p_3 (or p_4):

$$p_3 = -\frac{2\pi u_0}{\omega}, \quad p_4 = \frac{2\pi u_0}{\omega} \quad (2.6)$$

(Figs. 1c, d). Both waves have the same phase velocity, equal to u_0 :

$$v_{ph3} = v_{ph4} = u_0 \quad (2.7)$$

(this is why these waves are called synchronous).

An observer located on a fixed plane $z = \text{const}$ will see the motion of the trace left by the beam penetrating through this plane. For waves a_1 and a_3 this trace rotates counterclockwise with frequency ω , while for a_2 and a_4 —clockwise with the same frequency. Thus, the waves a_1 and a_3 have negative or left-hand circular polarization, while a_2 and a_4 are positively (right-hand) polarized.* The motion of the excited beam can always be represented as a superposition of the transverse waves a_1, \dots, a_4 , given by (1.12) and (1.13). The kinematics of the center of inertia of the beam cross section can be quite complicated [25].

The kinetic power of the transverse waves is given by

$$P_j = \sigma_j \frac{\omega}{\omega_c} |a_j|^2, \quad j=1, 2, 3, 4, \quad (2.8)$$

$$\sigma_1 = \sigma_4 = 1, \quad \sigma_2 = \sigma_3 = -1. \quad (2.9)$$





Since a_3 carries negative kinetic power and the a_4 has positive power, they are arbitrarily called slow and fast synchronous waves, respectively, although both have the same phase velocity u_0 .

The kinetic power P_j of the transverse waves is made up of the longitudinal-motion power P_{Lj} and the transverse-motion power P_{Tj} [26,27]:

$$P_j = P_{Lj} + P_{Tj} \quad (j=1, 2, 3, 4). \quad (2.10)$$

*Opposite definitions are sometimes used for the polarization directions.

Table I. Characteristics of transverse waves of an electron beam

Wave	Designation	Polarization	β	P_{kin}	P_t	P_i
Fast cyclotron	a_1		$\beta_e - \beta_c$	$\frac{\omega}{\omega_c} a_1 ^2$	$ a_1 ^2$	$\left(\frac{\omega}{\omega_c} - 1\right) a_1 ^2$
Slow cyclotron	a_2		$\beta_e + \beta_c$	$-\frac{\omega}{\omega_c} a_2 ^2$	$ a_2 ^2$	$-\left(\frac{\omega}{\omega_c} + 1\right) a_2 ^2$
Slow synchronous	a_3		β_e	$-\frac{\omega}{\omega_c} a_3 ^2$	0	$-\frac{\omega}{\omega_c} a_3 ^2$
Fast synchronous	a_4		β_c	$\frac{\omega}{\omega_c} a_4 ^2$	0	$\frac{\omega}{\omega_c} a_4 ^2$

The longitudinal power is due to the longitudinal electric field, which is always present off the axis or at the edges of the devices that excite the transverse waves, owing to the inhomogeneity of the transverse field^[24]. Indeed, let, for example, the field \mathbf{E} be produced by a transmission-line wave propagating along the z axis with frequency ω and phase constant β . Since the waves are slow, that is, $\beta \gg \omega/c$, we find from the third Maxwell equation that $\text{curl } \mathbf{E} = 0$, and

$$\frac{\partial E_z}{\partial x} = \frac{\partial E_x}{\partial z} = -i\beta E_x, \quad \frac{\partial E_z}{\partial y} = \frac{\partial E_y}{\partial z} = -i\beta E_y. \quad (2.11)$$

Using (2.11), we can find the increment of E_z for small displacements $\Delta x = x$ and $\Delta y = y$ from the beam equilibrium position (system axis), assuming that $E_z = 0$ in the equilibrium position:

$$E_z = \frac{\partial E_x}{\partial x} \Delta x + \frac{\partial E_y}{\partial y} \Delta y = -i\beta (E_x x + E_y y) \neq 0. \quad (2.12)$$

The transverse power of both cyclotron waves is positive^[24,27]:

$$P_{ij} = |a_j(\omega)|^2 \quad (j=1, 2); \quad (2.13)$$

The longitudinal power is

$$P_{11}(\omega) = \left(\frac{\omega}{\omega_c} - 1\right) |a_1(\omega)|^2, \\ P_{12}(\omega) = -\left(\frac{\omega}{\omega_c} + 1\right) |a_2(\omega)|^2 \quad (2.14)$$

(The bar denotes averaging over the ensemble of realizations of the process in the usual sense^[28].) In synchrotron waves, the electrons do not have transverse velocities, and therefore $P_{t3} = P_{t4} = 0$ and the kinetic power consists only of the longitudinal-motion power. The main characteristics of transverse waves are listed in Table I.

3. MECHANISM OF PARAMETRIC AMPLIFICATION

We shall analyze the construction and operating principle of electron parametric amplifiers (EPA) using as an example the fast cyclotron wave ampli-

fier, first described by R. Adler in 1958^[29-31]. In this amplifier (Fig. 4) the electron beam passes in succession through an input unit 1 tuned to the signal frequency ω_s , a pump resonator 2 tuned to the frequency ω_p , and an output unit 3 tuned to ω_s . The input (output) unit is a cavity with an interaction space in the form of a capacitive gap, in which the electric field is perpendicular to the electron beam (transverse-field cavity^[32,33]). In the input cavity the noise power of the fast cyclotron wave is removed from the beam and is dissipated in the active resistances of the input unit. At the same time there are introduced into the beam the amplified signal, the external noise (antenna noise), and the internal thermal noise of the cavity, which causes transverse-velocity modulation of the electron beam.

The signal is amplified in the pump field. It can be shown that amplification of transverse waves of an electron beam is possible in any inhomogeneous transverse electric field^[34]. However, in order for the amplification to be linear in the case of small signals, that is, in order for the gain to be constant and independent of the input-signal amplitude, the field intensity near the axis should depend linearly on the transverse coordinates x and y .

Such a field can be produced, for example, by a quadrupole capacitor—four electrodes of hyperbolic form under potentials $\pm V_p$. The equipotential lines of the field are hyperbolas (Fig. 5). However, even if the electrodes are not strictly hyperbolic in shape (say, round), the field near the axis is sufficiently close to hyperbolic^[35]. In Adler's tube the pump electrodes are fed from the pump generator (Fig. 6a) and have potentials $V_p = \pm V_{pm} \cos \omega_p t$, producing a transverse field of the type shown in Fig. 5 and of frequency ω_p .

The mechanism of amplification can be explained by considering an electron situated at the instant $t = 0$ at the point A (see Fig. 5) and revolving with frequency ω_c in a direction indicated by the arrow. The electron is accelerated by the electric field and

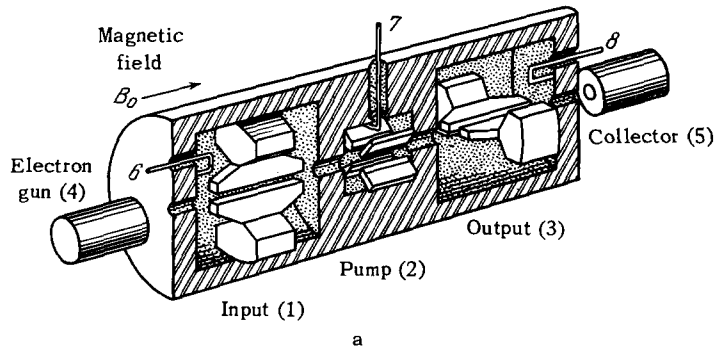


FIG. 4. Construction (a) and operating principle (b) of an EPA of the Adler type. 1 - Input coupling unit; 2 - pump region; 3 - output coupling unit; 4 - gun; 5 - collector; 6 - signal input; 7 - pump input; 8 - amplified signal output; 9 - intermediate noise waves produced by the gun; 10 - fast cyclotron noise wave; 11 - noise power output.

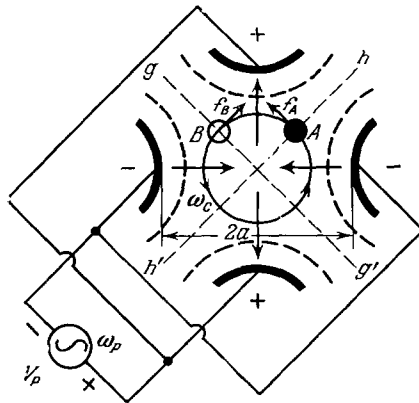
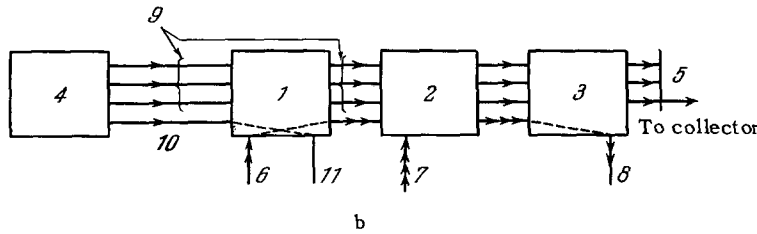


FIG. 5. Field of quadrupole capacitor. gg' , hh' - zero equipotentials; f_a , f_b - forces acting on the electrons at the points A and B.

its transverse velocity increases. If $\omega_p = 2\omega_c$, then the electron reaches after one-quarter of a revolution the point B, the field reverses sign, the electron is again accelerated, etc. This leads to an increase in the electrons radius of revolution, that is, to signal amplification at the expense of the pump power. Inasmuch as the pump field that acts on the electron and increases the radius of its revolution is parametric, with frequency $\omega_p = 2\omega_c$, the amplification is parametric. If at the instant $t \approx 0$ the electron is situated at the point B, then the field will cause it to be decelerated. The effect of the quadrupole is thus to produce exponentially rising and falling waves.

The amplified signal is picked off by an output cavity similar to the input cavity. The prior elimination of the fast-wave noise makes it possible to obtain a very low amplifier noise figure. An amplifier of this type has the lowest noise figure of all the presently known microwave electron beam amplifiers.

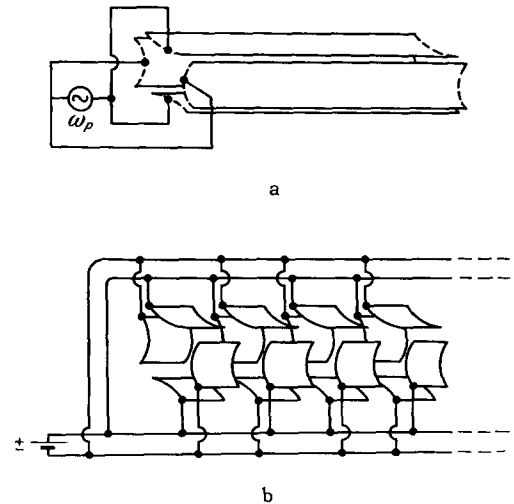


FIG. 6. Adler's quadrupole with solid (a) and sectionalized plates (b).

By way of another example, let us consider an electrostatic amplifier (ESA) with sectionalized quadrupole (Fig. 6b)^[36]. It differs from Adler's amplifier only in the pump field, which in this case is electrostatic and varies along the z axis like $\cos \beta_p z$. If the pitch of the quadrupole, that is, the distance between sections, is chosen such that during one-quarter of a revolution the electron has time to move to the next section, the amplification mechanism can be illustrated with the aid of the same figure 5.

A detailed analysis shows^[37] that in an ESA the electrons move perpendicular to the force lines of the transverse electric field, remaining on one equipotential. Thus, these forces perform no work, and the energy necessary for the amplification is supplied here not by the electrostatic field but by the electron

beam itself. As shown in Sec. 2, a longitudinal electric field exists outside the quadrupole axis. Under the influence of this field, some of the electrons are slowed down. Then the ESA amplifies to an equal degree one of the slow waves with negative kinetic power, besides the fast wave of the beam, so that the total kinetic power of the beam is conserved. Active coupling with the slow wave increases the noise figure of such amplifiers above the level expected of low-noise amplifiers.

We now investigate the amplification mechanism with greater rigor. We assume that the pump generator (wave) power greatly exceeds the power of the transverse waves of the beam, so that in this region we can neglect the reaction of the beam on the pump field (in particular, we can disregard the possibility of saturation of the pump generator, the induced currents, and similar effects).

We express the pump field in the form

$$U_p(x, y, z) = \text{Re} [V_p \Phi_p(x, y, z)], \quad (3.1)$$

where U_p —potential in the region where the beam passes, V_p —potential of the pump electrodes, and $\Phi_p(x, y, z)$ —some function of the coordinates, depending on the type of the pump structure.

The pump field intensity is

$$\left. \begin{aligned} E_{px} &= -\frac{\partial U_p}{\partial x} = -\text{Re} [V_p \Phi'_{px}(x, y, z)], & \Phi'_{px} &\equiv \frac{\partial \Phi_p}{\partial x}, \\ E_{py} &= -\frac{\partial U_p}{\partial y} = -\text{Re} [V_p \Phi'_{py}(x, y, z)], & \Phi'_{py} &\equiv \frac{\partial \Phi_p}{\partial y}. \end{aligned} \right\} (3.2)$$

The configuration of the pump electrodes is chosen such that Φ'_{px} and Φ'_{py} depend linearly on x and y . For the quadrupole shown in Fig. 5

$$\Phi_p(x, y, z) = \frac{1}{2a} (x^2 - y^2), \quad (3.3)$$

where $2a$ is the distance between plates.

We represent the potential of the pump electrodes in a rather general form:

$$\text{Re } V_p = V_{pm} \cos(\omega_p t - \beta_p z) = \frac{V_{pm}}{2} [e^{i(\omega_p t - \beta_p z)} + e^{-i(\omega_p t - \beta_p z)}], \quad (3.4)$$

where β_p is the propagation constant, while $\beta_p > 0$ and $\beta_p < 0$ corresponds to the forward and to the backward pump waves. In Adler's tube $\beta_p = 0$, while in an ESA $\omega_p = 0$ and $\beta_p \neq 0$. For generality we can introduce also an initial phase φ_0 , that is, we can put $\text{Re } V_p = V_{pm} \cos(\omega_p t - \beta_p z + \varphi_0)$.

The equations of beam motion in a specified pump field are^[36]

$$\begin{aligned} & \left(\frac{\partial}{\partial t} + u_0 \frac{\partial}{\partial z} - i\omega_c \right) a_1 \\ &= -i \frac{\Omega^2}{\omega_c} (a_4 - a_2) [e^{i(\omega_p t - \beta_p z)} + e^{-i(\omega_p t - \beta_p z)}], \\ & \left(\frac{\partial}{\partial t} + u_0 \frac{\partial}{\partial z} + i\omega_c \right) a_2 = i \frac{\Omega^2}{\omega_c} (a_3 - a_1) [e^{i(\omega_p t - \beta_p z)} + e^{-i(\omega_p t - \beta_p z)}], \\ & \left(\frac{\partial}{\partial t} + u_0 \frac{\partial}{\partial z} \right) a_3 = -i \frac{\Omega^2}{\omega_c} (a_4 - a_2) [e^{i(\omega_p t - \beta_p z)} + e^{-i(\omega_p t - \beta_p z)}], \\ & \left(\frac{\partial}{\partial t} + u_0 \frac{\partial}{\partial z} \right) a_4 = i \frac{\Omega^2}{\omega_c} (a_3 - a_1) [e^{i(\omega_p t - \beta_p z)} + e^{-i(\omega_p t - \beta_p z)}], \end{aligned} \quad (3.5)$$

$$\Omega^2 = \frac{|e| V_{pm}}{ma^2} (\text{sec}^{-2}) \quad (3.6)$$

($\Omega^2 =$ parameter of the pump field intensity). We see from (3.5) that in the presence of a pump field ($\Omega^2 \neq 0$) any wave a_j can be a source of waves of all other types. From (3.5) it follows also that if any of the waves varies like $\exp[i(\omega t - \beta z)]$, then there appear on the right sides of the equations harmonics with frequencies ($\omega \pm \omega_p$) and propagation constants ($\beta \pm \beta_p$), which in turn give rise to new harmonics, etc. Thus, an entire series of waves is produced, with frequencies and propagation constants*

$$\omega_n = \omega + n\omega_p, \quad \beta_n = \beta + n\beta_p \quad (n=0, \pm 1, \pm 2, \dots). \quad (3.7)$$

In accordance with this, the solution will be sought in the form

$$a_j = \sum_{n=-\infty}^{\infty} a_{j,n}(z) e^{i(\omega_n t - n\beta_p z)}, \quad j=1, 2, 3, 4. \quad (3.8)$$

For generality we assume here that each of the harmonics $a_{j,n}$ has its own z -dependence.

Substituting (3.8) in (3.5) and equating terms with identical t -dependence, we obtain^[36]

$$\begin{aligned} & \left(-i \frac{\partial}{\partial z} + \frac{\omega_n - \omega_c - n\beta_p u_0}{u_0} \right) a_{1,n} \\ &+ \frac{\Omega^2}{\omega_c u_0} (a_{4,n-1} - a_{2,n-1} + a_{4,n+1} - a_{2,n+1}) = 0, \\ & \left(-i \frac{\partial}{\partial z} + \frac{\omega_n + \omega_c - n\beta_p u_0}{u_0} \right) a_{2,n} \\ &- \frac{\Omega^2}{\omega_c u_0} (a_{3,n-1} - a_{1,n-1} + a_{3,n+1} - a_{1,n+1}) = 0, \\ & \left(-i \frac{\partial}{\partial z} + \frac{\omega_n - n\beta_p u_0}{u_0} \right) a_{3,n} \\ &+ \frac{\Omega^2}{\omega_c u_0} (a_{4,n-1} - a_{2,n-1} + a_{4,n+1} - a_{2,n+1}) = 0, \\ & \left(-i \frac{\partial}{\partial z} + \frac{\omega_n - n\beta_p u_0}{u_0} \right) a_{4,n} \\ &- \frac{\Omega^2}{\omega_c u_0} (a_{3,n-1} - a_{1,n-1} + a_{3,n+1} - a_{1,n+1}) = 0. \end{aligned} \quad (3.9)$$

This system has the same form as (1.24) with infinite matrix R .

Figure 7 illustrates the coupling between different modes in accordance with (3.9). The solid lines show active coupling while the dashed lines show passive coupling. The diagram continues to infinity on the right and on the left. The points a and a' , b and b' , etc., must be imagined as coinciding by wrapping the diagram into a cylinder. On the right are indicated the signs of the kinetic power σ_j in accordance with (2.9), inasmuch as the power of the n -th harmonic is

$$P_{j,n} = \sigma_j \frac{\omega_n}{\omega_c} |a_{j,n}|^2. \quad (3.10)$$

*Harmonics of the type $\omega_{m,n} = m\omega + n\omega_p$ do not appear, because the beam modes at frequencies $\omega + n\omega_p$ have small power in the small-signal approximation and do not lead to a noticeable formation of harmonics with the beam wave at frequency ω . In the case of large signals, such harmonics do appear. This makes it possible to use the tube as a frequency converter (Sec. 7).

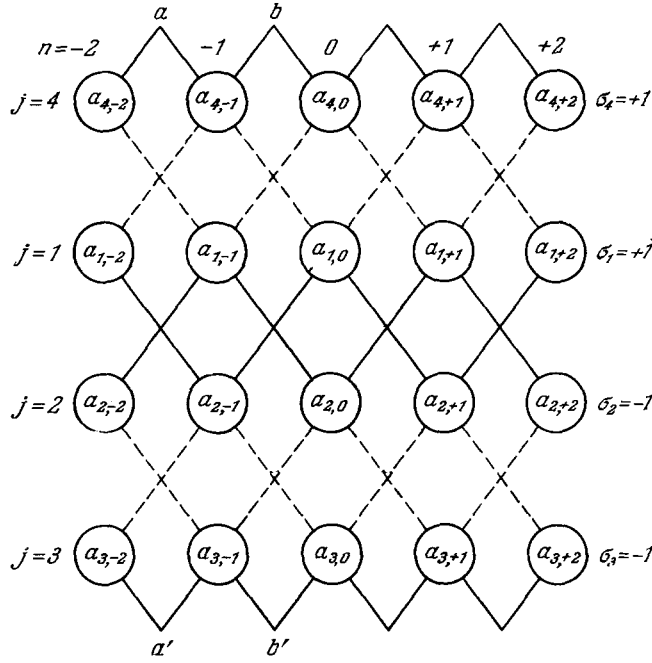


FIG. 7. Coupling between different modes in the amplification region.

We see that the actively coupled modes are those with different σ_j , and the passively coupled modes have the same σ_j .^{*} The meaning of the positive and negative frequencies is indicated in Sec. 2. Thus, for example, when $\omega_p > \omega$ the wave $a_{2,-1}$ is a fast cyclotron wave, since its kinetic power, defined in accordance with (3.10), is positive; when $\omega_p < \omega$, the wave $a_{2,-1}$ is a slow cyclotron wave. In analogy with (2.5), we have for the harmonics

$$a_{1,n}(-\omega) = a_{2,n}^*(\omega), \quad a_{3,n}(-\omega) = a_{4,n}^*(\omega). \quad (3.11)$$

For strong parametric coupling of any two modes with frequencies ω_1 and ω_2 and with propagation constants β_1 and β_2 , the following conditions must be satisfied^[38]

$$\omega_1 + \omega_2 = \omega_p, \quad (3.12)$$

$$\beta_1 + \beta_2 = \beta_p. \quad (3.13)$$

(For the quantities contained in the formulas, we admit of positive and negative values.) The condition (3.12) signifies that the corresponding modes should have a forward coupling on the diagram of Fig. 7. It follows from (3.13) that for strongly coupling modes the diagonal elements of the matrix of the system (3.9) should coincide (be close to one another). For an amplifier of the Adler type, the principal coupling is the strong coupling between the fast cyclotron waves $a_{1,0}$ (signal mode at frequency $\omega = \omega_s$) and $a_{2,-1}$ (idler mode at frequency $\omega_i = |\omega - \omega_p|$). For an amplifier with sectionalized quadrupole, the principal coupling is also between $a_{1,0}$ and $a_{2,-1}$, but now

^{*}This property is general and is established in the theory of coupled modes^[11].

$a_{2,-1}$ is a slow cyclotron wave at the signal frequency. Confining ourselves in (3.9) to the equations for these two waves only, and taking (3.8) into account, we obtain in both cases^[39]

$$\frac{\partial \mathbf{a}}{\partial z} = -iR\mathbf{a}, \quad \mathbf{a} = \begin{pmatrix} a_1(z, \omega) \\ a_2(z, \omega - \omega_p) \end{pmatrix},$$

$$R = \begin{pmatrix} \beta_1(\omega), & -k(\omega)e^{-i\beta_p z} \\ k^*(\omega)e^{i\beta_{1z}}, & \beta_2(\omega - \omega_p) \end{pmatrix}, \quad (3.14)$$

$$\beta_1(\omega) \equiv \frac{\omega - \omega_c}{u_0}, \quad \beta_2(\omega - \omega_p) \equiv \frac{\omega + \omega_c - \omega_{pe}}{u_0}, \quad k(\omega) = \frac{\Omega^2}{\omega_c u_0}. \quad (3.15)$$

Here $k(\omega)$ —coupling coefficient (written in general form), $\omega_{pe} \equiv (\omega_p - \beta_p u_0)$ —effective (Doppler-shifted) pump frequency, that is, the frequency which will be observed in the coordinate system moving with the electron velocity u_0 .

The eigenvalues γ of the matrix R , that is, the propagation constants of the signal mode $a_1(z, \omega)$ and the idler mode $a_2(z, \omega - \omega_p)$, are

$$\gamma_{1,2} = \beta \pm i\xi, \quad \beta \equiv \frac{\beta_1(\omega) + \beta_2(\omega - \omega_p)}{2} = \frac{2\omega - \omega_{pe}}{2u_0},$$

$$\xi \equiv \left(|k|^2 - \left(\frac{\Delta\beta}{2} \right)^2 \right)^{1/2}, \quad (3.16)$$

where

$$\Delta\beta \equiv \beta_1(\omega) - \beta_2(\omega - \omega_p) = (\omega_{pe} - 2\omega_c)/u_0^*.$$

Growing waves are possible when

$$|\omega_{pe} - 2\omega_c| < \frac{2\Omega^2}{\omega_c}. \quad (3.17)$$

The weaker the pumping, that is, the smaller Ω^2 , the closer ω_{pe} and $2\omega_c$ should be for the active coupling to exist. The minimum amplification will occur when

$$\omega_{pe} = 2\omega_c. \quad (3.18)$$

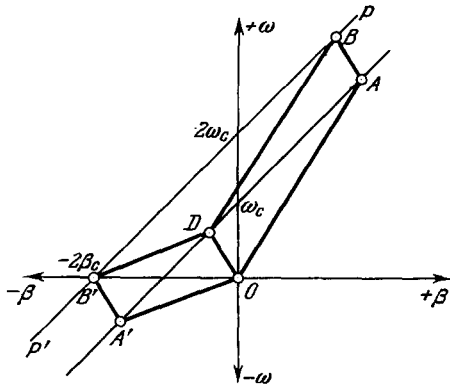
In this case

$$\gamma_{1,2} = \frac{\omega - \omega_c}{u_0} \pm i \frac{\Omega^2}{\omega_c u_0} \quad (3.19)$$

and the gain is proportional to Ω^2 , that is, to the pump voltage. Figure 8 shows an $\omega - \beta$ -diagram for this case. The line pp' represents the formula $\omega_p = 2\omega_c + \beta_p u_0$; the point D corresponds to the signal mode, A to the idler mode, and B to the pump mode for the chosen operating condition. In Adler's amplifier $\beta_1 = \beta_p = 0$ and the parallelogram OABD degenerates into the segment $[0, 2\omega_c]$ on the ordinate axis. In the ESA $\omega_p = 0$; for this case the $\omega - \beta$ diagram is represented by the parallelogram OA'B'D.

^{*}An analogous analysis for the case of active coupling between $a_{2,0}$ (slow cyclotron wave of the signal) and $a_{1,1}$ (fast cyclotron wave at frequency $\omega + \omega_p$) leads to a value

$$\gamma = \frac{2\omega + \omega_{pe}}{2u_0} \pm i\xi.$$

FIG. 8. ω - β diagram with pumping.

The solution of (3.14) takes the form [39]

$$\begin{aligned}
 a_1(z, \omega) &= \left[\left(\text{ch } \xi z - i \frac{\Delta\beta}{2\xi} \text{sh } \xi z \right) a_1(0, \omega) \right. \\
 &\quad \left. - i \frac{k}{\xi} \text{sh } \xi z \cdot a_2(0, \omega - \omega_p) \right] e^{-i\beta z}, \\
 a_2(z, \omega - \omega_p) &= \left[i \frac{k^*}{\xi} \text{sh } \xi z \cdot a_1(0, \omega) \right. \\
 &\quad \left. + \left(\text{ch } \xi z + i \frac{\Delta\beta}{2\xi} \text{sh } \xi z \right) a_2(0, \omega - \omega_p) \right] e^{-i\beta z}. \quad (3.20)^*
 \end{aligned}$$

If $a_2(0, \omega - \omega_p) = 0$, then we have for the powers

$$\begin{aligned}
 P_1(z, \omega) &\equiv \frac{\omega}{\omega_c} |a_1(z, \omega)|^2 = \left(1 + \frac{|k|^2}{\xi^2} \text{sh}^2 \xi z \right) P_1(0, \omega), \\
 P_1(0, \omega) &\equiv \frac{\omega}{\omega_c} |a_1(0, \omega)|^2, \\
 P_2(z, \omega - \omega_p) &\equiv - \frac{\omega - \omega_p}{\omega_c} |a_2(z, \omega - \omega_p)|^2 \\
 &= \frac{\omega_p - \omega}{\omega} \frac{|k|^2}{\xi^2} \text{sh}^2 \xi z P_1(0, \omega). \quad (3.21)
 \end{aligned}$$

Figure 9 shows curves of the relative power, constructed from formulas (3.21), for the case of complete synchronism (3.18) and for the case when there are no growing solutions. Figure 10 shows the rela-

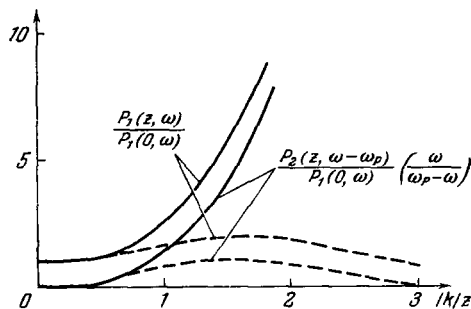


FIG. 9. Relative power of the signal and idler modes in the amplification region for the case of complete synchronism (solid lines) and for the case when there are no growing solutions (dashed lines)

$$-\Delta\beta=0, \quad - \frac{\Delta\beta}{2k} = \sqrt{2}.$$

*sh \equiv sinh, ch \equiv cosh.

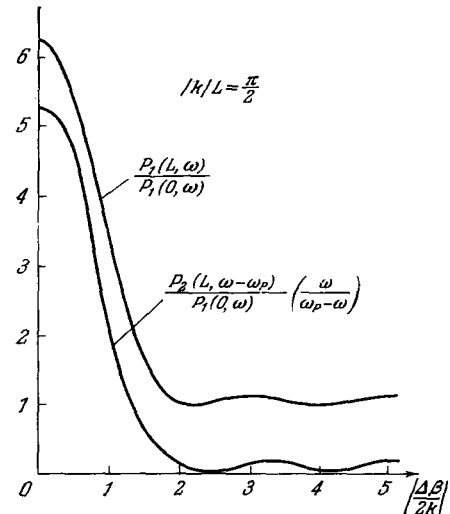


FIG. 10. Relative power of signal and idler modes at the output from the quadrupole as a function of the degree of non-synchronism.

tive power of the signal mode and of the idler mode at the outputs of the quadrupole line $L = \pi/2 |k|$, as a function of the degree of deviation from synchronism $|\Delta\beta/(2k)|$.

It follows from (3.20) that

$$\left. \begin{aligned}
 \frac{\partial}{\partial z} \left(\frac{P_1(z, \omega)}{\omega} + \frac{P_2(z, \omega - \omega_p)}{\omega - \omega_p} \right) &= 0, \\
 \frac{P_1(L, \omega)}{\omega} + \frac{P_2(L, \omega - \omega_p)}{\omega - \omega_p} &= \frac{P_1(0, \omega)}{\omega} + \frac{P_2(0, \omega - \omega_p)}{\omega - \omega_p}. \quad (3.22)
 \end{aligned} \right\}$$

The conservation laws (3.22) are called the Manley-Rowe relations [40]. It is seen from these relations that the power carried by the signal and idler modes is proportional to their frequencies $\omega_s = \omega$ and $\omega_i = |\omega - \omega_p|$. The power P_p delivered by the pump generator is

$$\begin{aligned}
 P_p &= P_1(L, \omega) + P_2(L, \omega - \omega_p) \\
 &\quad - [P_1(0, \omega) + P_2(0, \omega - \omega_p)] \\
 &= \frac{\omega_p}{\omega} [P_1(L, \omega) - P_1(0, \omega)]. \quad (3.23)
 \end{aligned}$$

With decreasing ratio ω_p/ω , the power P_p decreases. In electrostatic amplifiers $\omega_p = 0$, and therefore $P_p = 0$.

We can consider analogously the amplification process by retaining in (3.9) all the harmonics with which the signal mode $a_{1,0}$ is directly coupled on the diagram of Fig. 7, that is, $a_{1,0}$, $a_{2,-1}$, $a_{3,-1}$, and $a_{4,0}$ [11]. In this case we can find four propagation constants, two of which give growing and attenuating waves due to the active coupling between $a_{1,0}$ and $a_{2,-1}$, and two correspond to periodic solutions due to the passive coupling of the cyclotron waves $a_{1,0}$ and $a_{2,-1}$ with the synchronous waves $a_{3,-1}$ and $a_{4,0}$. The Manley-Rowe relations for this case are*

*The Manley-Rowe relations are established in general form in the theory of coupled modes as one of the invariant quadratic forms [12, 13].

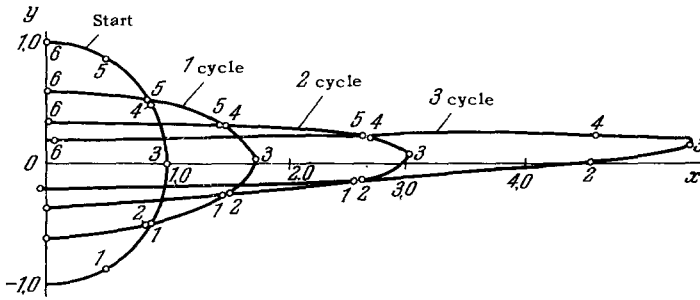


FIG. 11. Increase in the phase bunching in the quadrupole in each succeeding revolution cycle.

$$\frac{\partial}{\partial z} \left(\frac{P_{1,0}}{\omega} + \frac{P_{3,0}}{\omega} + \frac{P_{2,-1}}{\omega - \omega_p} + \frac{P_{3,-1}}{\omega - \omega_p} \right) = 0. \quad (3.24)$$

As shown in [41] by the method of [26], if the pump parameter Ω^2 is sufficiently large, harmonics at frequencies $\pm(\omega + \omega_p)$ can be amplified in addition to the transverse velocities at the signal frequency ω . With further increase in Ω^2 , the harmonics $\pm(\omega + 2\omega_p)$ can be amplified, etc. The signal gain depends on how the input power of the signal is distributed among the different modes excited in the pump region. If we assume that at the input to the quadrupole only one signal wave $a_{1,0}$ is excited, then we obtain from (3.21) for the case $\Delta\beta = 0$ and $\cosh^2 |k|L \gg 1$ [4,11]

$$\left. \begin{aligned} G &= 27.3\alpha N_q - 6[\text{db}], \\ \alpha &\equiv \frac{2\Omega^2}{\omega_p^2}, N_q \equiv \frac{\beta_c L}{2\pi}, \end{aligned} \right\} \quad (3.25)$$

where N_q —number of cyclotron waves subtended by the length L of the quadrupole.

The trajectories of the electrons in the quadrupole depend on the phase of their entry into the pump region. Figure 11 shows the position of different electrons 1, 2, 3, ... in a coordinate system rotating with frequency $\omega = \omega_p/2$ and moving in translation with velocity u_0 ($\beta_p = 0$). By virtue of the symmetry, we show only the electrons having $x \geq 0$. At the initial instant the electrons are uniformly distributed over the entrance phases, but as they move through the pump region they are gradually bunched near the most favorable phase that ensures maximum gain [42]. Obviously, a beam of round cross section with noise-modulated transverse velocities will acquire under the influence of this mechanism a shape reminiscent of a two-blade propeller rotating with frequency ω .

4. INPUT (OUTPUT) DEVICE FOR COUPLING WITH THE FAST CYCLOTRON WAVE

The input (output) couplers influence the most important characteristics of parametric amplifiers. Thus, for example, it has been established theoretically and experimentally that electronic amplification in the quadrupole (3.25) does not depend on the signal frequency ω_s [30,43]. The bandwidth of the tube is therefore determined exclusively by the frequency characteristics of the power exchange between the antenna and the beam in the input coupler and be-

tween the beam and the load in the output unit. The couplers also determine the total gain of the tube (the electronic gain of the tube minus the losses in the input and output units) and the output saturation power, and consequently also the dynamic range of the amplifier. In EPA for fast cyclotron waves, the couplers determine also the minimum noise figure, which depends primarily on the efficiency with which the noise power is removed from the beam in the input unit.

Couplers of the capacitor type [32,43a] operate at near-cyclotron frequency, $\omega_s \approx \omega_c$. For the fast cyclotron wave we have $\beta_1 \approx 0$ and $v_{ph1} \approx \infty$. If the length of the capacitor plates l is small compared with the signal wavelength ($l \ll 2\pi c/\omega_s$), then the phase of the electric field is the same at all points of the capacitor gap, that is, the phase velocity of the system is $v_{ph.s} \approx \infty$. We can therefore analyze the operation of the input coupler by representing it in the form of a circuit with lumped parameters.

When the electrons move in the capacitor, the signal field in the capacitor increases the radius of their revolution. When $\omega_s = \omega_c$, the beam excited in the fast cyclotron mode follows the generatrix of a cone; this generatrix rotates with frequency ω_c around the z axis. When $\omega_s \neq \omega_c$ the electron trajectory assumes the form of a helix with increasing radius. If the gap is sufficiently long, beats are produced, since the revolution of the electrons gradually falls out of synchronism with the field of the signal in the capacitor [44].

Near the cyclotron frequency we can neglect the slow cyclotron and synchrotron waves* and investigate the operation of the input coupler with the aid of the equivalent circuit of Fig. 12 [46]. In the figure, G_e and B_e are the active and reactive components of the electronic admittance of the beam, $Y_e = G_e + iB_e$; G_c and B_c are the components of the admittance of the input coupler (cavity), $Y_c = G_c + iB_c$;

*Near $\omega_s = \omega_c$ the slow cyclotron wave of the noise passes through the resonator practically without change. The synchronous waves are not coupled in a homogeneous field with the cyclotron waves. However, the inhomogeneity of the field on the edges of the capacitor can cause the noise of the synchronous waves to be transferred to the fast cyclotron wave and deteriorate the noise figure of the amplifier. It is therefore desirable to reduce these inhomogeneities and their influence [45].

G_L and B_L are the admittance components of the signal source (antenna). Usually $G_C \ll G_L$ and $B_C \gg B_L$; the electronic admittance of the gap (G_e, B_e) is a known function of the frequency and of the parameters of the coupler, and can be found in several papers [43,46]. The input noises of the beam are described by means of a noise generator $i_e^2 = 4kT_e G_e \Delta f$, where T_e is the electronic transverse noise temperature and Δf is the frequency band. This noise enters through arm 1 into the circulator C, is partially (or completely) dissipated in the cavity and in the antenna (arm 2), and is partially again reflected into the electron beam (arm 3). The signal, the antenna noise (external noise), and the intrinsic noise of the cavity, which are produced respectively by the current generators $i_s^2, i_L^2 = 4kTG_L \Delta f$, and $i_C^2 = 4kT_0 G_C \Delta f$ (T —antenna (input) temperature and T_0 —cavity temperature) are simultaneously introduced into the beam. An analogous diagram can be drawn also for the output coupler.

From the circuit of Fig. 12 we can find the equivalent noise temperature T_N of the fast cyclotron wave of the beam at the entrance to the amplification region, which we define as the load temperature $T = T_N$ at which the total noise power going into the arm 3 has double the value at the temperature $T = 0$ [46]:

$$\frac{T_N}{T_e} = \frac{(G_L + G_c - G_e)^2 + (B_L + B_c + B_e)^2}{4G_L G_e} + \frac{T_0}{T_e} \frac{G_e}{G_L}. \quad (4.1)$$

The first term in (4.1) represents the electron-beam noise reflected back to the beam in arm 2, and the second term represents the intrinsic cavity noise. Since $T_0 \ll T_t$, the second term can be neglected. At the frequency $\omega_s = \omega_c$ the condition of conjugate matching should be satisfied

$$Y_e(\omega_s) = Y_r^*(\omega_s), \quad Y_r \equiv Y_c + Y_L. \quad (4.2)$$

In this case $T_N = 0$, that is, the input noise (of the fast cyclotron wave) is completely removed from the beam.*

Assuming that the input and output couplers are identical, we also find from the circuit of Fig. 12 that

$$\frac{P_{out}}{P_{out, match}} = \left[\frac{4G_L G_e}{(G_L + G_c + G_e)^2 + (B_L + B_c + B_e)^2} \right]^2 \approx \left(\frac{T_N}{T_e} + 1 \right)^2, \quad (4.3)$$

where P_{out} is the output power of the amplifier and $P_{out, match}$ is the output power when the matching conditions (4.2) are satisfied.

Figure 13 shows the results of calculations by means of formulas (4.1) and (4.3) for capacitive type cavities. In the figure ΔG is the drop in gain (in dB) compared with the matched gain (at synchronism, $\omega_s = \omega_c$), L is the normalized length of the plates and F_0 is the detuning:

*It must be noted that only the noise of the fast cyclotron wave at the frequency $\omega_s = \omega_c$ is removed from the beam. At the same time, the total noise energy of the electron beam remains practically unchanged [47,48].

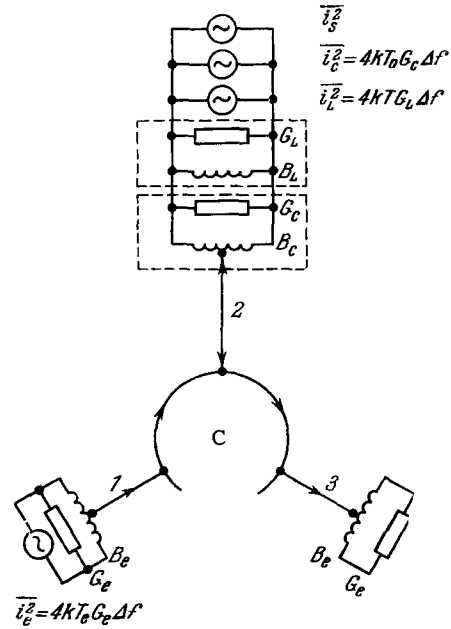


FIG. 12. Equivalent circuit of a cavity input coupler.

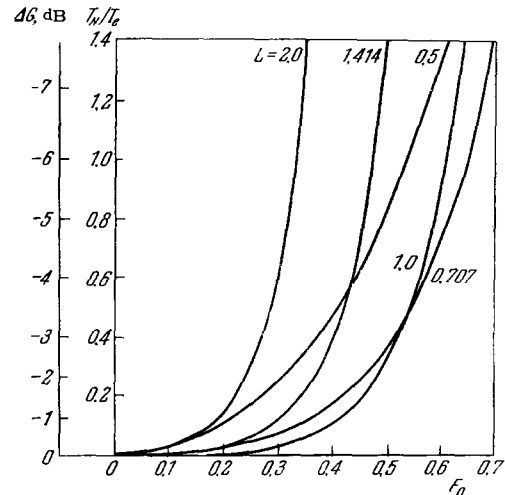


FIG. 13. Noise temperature and matching band of a cavity-type input coupler.

$$L = \frac{lv}{u_0}, \quad F_0 = \frac{\omega_s - \omega_c}{2\pi\nu}, \quad \nu = \sqrt{\frac{G_0 \mu_0}{48d^2 C}}, \quad (4.4)$$

l is the length of the plates, and C is the capacitance per unit length of the plates. As can be seen from the figure, the optimal values of L lie in the range 0.707–1.0.

It follows from (4.2) that the following condition must be satisfied for matching

$$B_e(\omega_s) = -B_r(\omega_s) \approx -B_c(\omega_s). \quad (4.5)$$

To broaden the frequency range of the amplifier, it is desirable to satisfy the condition (4.5) in a wider frequency band. As a rule, however, owing to the large plate capacitance, we have $|B_c(\omega_s)| > |B_e(\omega_s)|$ when $\omega_s \neq \omega_c$, which leads to a con-

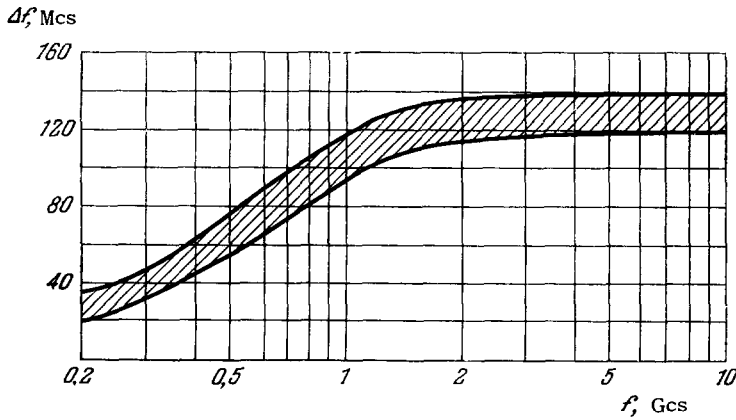


FIG. 14. Optimal band of resonator input unit.

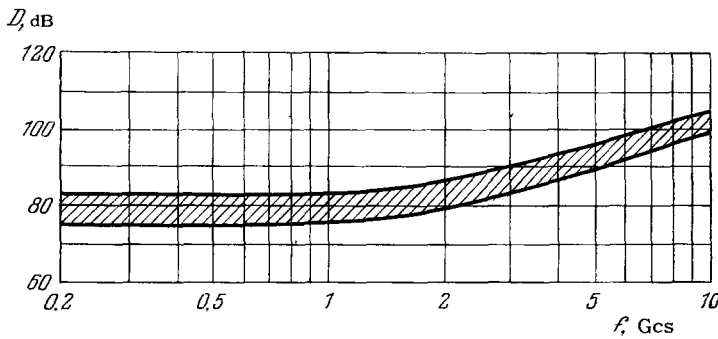


FIG. 15. Dynamic band of resonator input unit. Gain G = 20 dB.

siderable narrowing of the coupler matching band. The equivalent capacitance of the cavity can be reduced by using an external tuning circuit [43]. When (4.5) is satisfied, the matching bandwidth, that is, the frequency band in which $P_{out}/P_{out,match} \geq 1/2$, is approximately equal to $1/N$, where $N = \beta_c l/2$ is the number of cyclotron waves subtended by the gap L [43].

It has been shown theoretically that the frequency band in which the input noise of the fast cyclotron wave of the beam is removed can be broadened with the aid of additional cavities. These cavities are placed ahead of the input cavity and serve to remove the noise of the fast cyclotron wave in the vicinity of the frequency ω_c . With the aid of two additional cavities it is possible to broaden the noise-removal band by a factor 2–2.5 compared with the analogous single cavity [49].

If the electron orbit is so large following the amplification that the beam strikes the plates of the output cavity, saturation sets in. Saturation limits the maximum signal power which can still be amplified in the tube. The ratio of this power to the power of the minimally observed signal determines the dynamic range D of the amplifier:

$$D = 7.1 \cdot 10^3 \frac{I_0 f_c^2 (d - \delta_0)^2}{A_0 F}, \quad (4.6)$$

where I_0 is the beam current in amperes, f_c the cyclotron frequency in cps, A_0 the total gain, F the noise figure, and δ_0 the beam diameter in millimeters [43].

In Figs. 14 and 15, the shaded area indicates the

bandwidth and dynamic range (at a 20 dB gain) for an Adler tube with capacitive input coupler and with correctly chosen tube parameters [43].

A coupler for a fast cyclotron wave may also comprise a traveling-wave distributed device of the helix or ridge type with transverse field [26,50,51]. The propagation of the waves of the electron beam and of the line in such a system is described by an equation such as (1.24). For strong coupling between the fast cyclotron wave and the forward wave of the line, their phase constants should be equal in the middle of the pass band $\bar{\omega}_S$:

$$\beta_1(\bar{\omega}_s) = \beta_l(\bar{\omega}_s), \quad (4.7)$$

where β_l is the propagation constant of the line. Since $\beta_l(\bar{\omega}_s) > 0$, such couplers can be used only at frequencies $\omega_s > \omega_c$ (when $\omega_s < \omega_c$ operation with the backward wave of the line is possible [50].)

Inasmuch as both the forward wave of the system and the fast cyclotron waves carry positive power, a passive coupling exists between them, meaning a periodic exchange of energy. The minimum necessary line length l is chosen from the condition for complete mutual energy exchange between these modes [52,53]. Under certain simplifying assumptions we get

$$l = \frac{\pi}{2c(\bar{\omega}_s)}, \quad c(\bar{\omega}_s) = \Phi' \sqrt{\frac{\bar{\omega}_s G_0 Z_1(\bar{\omega}_s)}{8\omega_c}}. \quad (4.8)$$

Here c is the coupling coefficient, Z_l is the wave impedance of the line, and Φ' is determined from the relation $\Phi' = E_x/V_c$, where E_x is the transverse

field on the helix axis and V_C is the helix voltage.

The bandwidth of a coupler with known dispersion characteristics $\beta l(\omega_S)$ and $Zl(\omega_S)$ can be estimated approximately from the value of the coefficient (1.26), using the condition that at the limits of the band one must have

$$\left(\frac{\Delta\beta}{2}\right)^2 \approx c^2, \quad (4.9)$$

where $\Delta\beta = \beta_1 - \beta l$. For a line without dispersion, the bandwidth of the coupler unit does not exceed that of a cavity input coupler^[54]. The required line length, as that of a nonresonant structure, exceeds the length of the plates of a capacitive resonator, so that the bandwidth of the coupler is smaller. To increase the bandwidth it is desirable that the phase constant βl and the wave impedance Zl vary with frequency in the vicinity of $\overline{\omega_S}$ such that $\beta l(\omega_S) = \beta_1(\omega_S)$ and $\omega_S Zl(\omega_S) = \overline{\omega_S} Zl(\overline{\omega_S})$. In this case the bandwidth of the unit depends on the frequency region in which these relations are satisfied.

If the line has internal losses, the signal/noise ratio at the output of the coupler (in dB) is reduced by one-half the value of the total cold losses (in dB)^[54,55]. This is equivalent to a corresponding increase in the noise temperature. It must also be noted that in order to obtain a small noise figure it is usually necessary also to remove first the beam noise at the idler frequency $\omega_i = |\omega_S - \omega_p|$, which calls for an additional input coupler (see Sec. 7).

In Secs. 6 and 7 we shall indicate a few other devices for coupling with the fast cyclotron wave and with other transverse waves of the electron beam.

5. SOURCES OF AMPLIFIER NOISE

In fast-cyclotron-mode EPA, the slow mode of the beam does not participate in the amplification and is the main source of noise in ordinary (nonparametric) devices. Inasmuch as a correctly matched input coupler, eliminates completely the noise of the fast cyclotron wave at the signal frequency, one could expect the amplifier to have a noise figure $F = 1$ (0 dB). A noise figure 0.79–1.6 dB was attained in the best samples of foreign EPA, corresponding to a noise temperature 58–130°K. Of this total, 0.35–0.5 dB (25–30°K) is credited to losses in the input and output couplers^[30,56,57]. The causes of the remaining noise were at first unclear and were understood only after a more detailed investigation of the amplifier operation.

We note first that the published reports contain results of measurements of the so-called two-channel noise coefficient, that is, during the course of the measurement the noise from the source travels through both frequency channels, ω_S and $\omega_i = |\omega_S - \omega_p|$. Under real operating conditions, a signal is present only at the frequency ω_S , whereas the noise remains as before in both channels. In the quadru-

pole, owing to the strong coupling, the idler-mode noise ω_i goes over into the signal mode ω_S . If we neglect all the other noise sources, then as a result of this mechanism alone^[58]

$$F = 1 + \frac{\omega_S}{\omega_i} \frac{T_i}{T_0} \quad (T_0 = 290^\circ \text{K}), \quad (5.1)$$

where T_i is the equivalent noise temperature at the idler frequency ω_i . If $\omega_i = \omega_S$, the electron-beam noise at the frequency ω_i will be picked off in the input resonator together with the noise at the frequency ω_S . In this case T_i is the temperature of the external load or of the electrodes that produce the noise at the idler frequency ω_i . Assuming that $T_i = T_0$, we get $F = 2$. Thus when $T_i = T_0$, we must add to the figure obtained for the two-channel noise coefficient another 3 dB to obtain the real (single-channel) noise coefficient. We shall henceforth refer to the two-channel (measured) noise coefficient. The presence of the idler frequency is a shortcoming of parametric amplifiers as compared with ordinary nonparametric amplifiers.

A noise source inherent in the EPA is the presence of passively coupled modes. Thus, on the diagram of Fig. 7, slow synchronous waves at the signal frequency $a_{3,0}$ and at the idler frequency $a_{4,-1}$ are directly coupled with the signal mode $a_{1,0}$ and the idler mode $a_{2,-1}$. The slow-wave noise cannot be removed in principle in the input coupler, and goes over in the pump region into the signal mode. According to approximate estimates, the coupling with the $a_{3,0}$ and $a_{4,-1}$ modes increases the noise temperature by 10°K^[57]. If we take into account all the weakly coupled modes, their contribution to the noise temperature constitutes $2.70 \xi^2 T_K$, where ξ —amplification in nepers per radian of transit angle in the quadrupole (at frequency ω_C) and T_K is the cathode temperature. This temperature is of the order of 40°K^[36]. (With the aid of the general equation (3.9) we can investigate the influence of any number of harmonics; we need merely solve the equation numerically and retain the harmonics of interest, a laborious task.)

Synchronous waves are always present in the amplifier. In practice the beam is not infinitesimally thin, but has a finite diameter. Such a "thick" beam is always noise-modulated in all four modes $a_1, a_2, a_3,$ and a_4 . The spectral densities of these waves, for a thick beam leaving the gun, taking into account the shot noise and the space charge, were calculated by Blotekjaer^[59]. The noise of the synchronous modes a_3 and a_4 , as can be seen from (1.13), is made up of the noise of the transverse velocities and the noise of the transverse coordinates. The latter is subject to smoothing with a coefficient Γ^2 , where Γ^2 is the usual smoothing factor of shot noise due to the potential minimum near the cathode^[28]. The noise power is proportional to $(\omega/\omega_C) T_K$ for transverse velocities and to $\omega\omega_C T_K$ for the transverse

coordinates. The amplifier noise temperature estimated on the basis of these calculations greatly exceed the experimental results. Blotekjaer therefore assumes that some still unknown effect smooths out the noise.

J. Wessel-Berg and K. Blotekjaer have also established^[60] that if we take into account effects of second-order in Ω^2 , synchronous waves can become amplified in the quadrupole. These synchronous waves serve in turn as a source of a fast cyclotron wave, which is amplified even if the formulas of first-order of smallness in Ω^2 are used. Therefore an electron beam of finite diameter, broadens in the quadrupole even without noise or signal modulation. According to their estimates, this broadening can be the cause of saturation of amplification when the beam strikes the plates of the quadrupole and the noise increases sharply.

To reduce the coupling with the synchronous waves* it is recommended in both cases that the amplitude of the pump be reduced, and that the length of the quadrupole to obtain the same gain be increased accordingly^[36,60]. The noise coefficient is influenced somewhat also by lens effects in the amplifier^[36,47].

Let us consider next the role of space charge^[61,62]. If the beam moves in the drift region, then an arbitrary magnetic field and the radial field of space charge the beam cross section, produce an internal rotation of electrons with frequencies

$$\begin{aligned}\omega'_c &= \frac{\omega_c}{2} \left[1 - \sqrt{1 - 2 \left(\frac{\omega_q}{\omega_c} \right)^2} \right], \\ \omega''_c &= \frac{\omega_c}{2} \left[1 + \sqrt{1 - 2 \left(\frac{\omega_q}{\omega_c} \right)^2} \right],\end{aligned}\quad (5.2)$$

where $\omega_q = \eta\rho/\epsilon_0$ is the plasma frequency, and ρ_0 the space charge density. The frequency $\omega''_c \approx \omega_c$ describes the fast rotation of electrons and the frequency ω'_c slow rotation. The latter causes rotation of the beam as a whole, and the individual electrons move along complicated epicycloidal orbits.

In the input couplers, owing to the homogeneity of the capacitor gap field, the internal rotation of the electrons can be disregarded. In these couplers the signal field excites motion of the beam as a whole. In the quadrupole, however, the phenomena become more complicated. If the pump frequency is chosen to be $\omega_p = 2\omega'_c$, then signal amplification gives way to broadening of the orbits of the internal rotation of electrons, due to the space charge. An analogous phenomenon occurs when $\omega_p = 2\omega'_c$. When the space charge is small $\omega''_c \approx \omega_c$ and the rotation at the frequency ω''_c falls in the amplification band of the quadrupole. This raises the danger of untwisting of the internal orbits to such a degree that the electrons

begin to strike the plates of the quadrupole or of the output cavity. Experiments have shown that this effect can cause saturation of amplification, with simultaneous sharp increase of amplifier noise. In the case of large space charge ω''_c differs noticeably from ω_c and no such effect takes place, so that a large gain is obtainable. In real tubes, owing to the large current density in the beam, the ratio ω_q/ω_c reaches 0.5.

The signal introduced into the beam in the input coupler is distributed among the individual layers of the beam, which move with slightly different velocities. This velocity difference produces a phase shift between these layers, proportional to the distance between the input and output couplers. This reduces the signal power that can be extracted in the output coupler, since the electron motions (induced current) in the output capacitor do not add up in phase. The noise reduction attainable in the input coupler likewise deteriorates, and noise reappears in the beam.

According to calculations by Gordon^[63], this effect does not come into play if the phase velocities of the fast cyclotron waves at frequencies ω_s and ω_i are infinite. This occurs when $\omega_s \approx \omega_i \approx \omega_c$. Such an amplifier is called degenerate (for example, an amplifier of the Adler type). In a nondegenerate amplifier, the signal frequency ω_s differs greatly, sometimes by a factor of several times, from the idler frequency ω_i . In this case at least one of the waves propagates with a finite phase velocity. In a nondegenerate amplifier, therefore, the noise comes noticeably into play because of the influence of the longitudinal-velocity scatter (Sec. 7), which also causes the electrons to acquire unequal energy in the pump region. This phenomenon occurs also in a degenerate amplifier, and according to Gordon's estimates its contribution to the noise temperature is of order $0.2-2^\circ\text{K}$ ^[63].

If the process of parametric amplification is based on passive coupling with the slow wave of the electron beam (this takes place, for example, in an ESA), then the minimum noise figure of such a device is determined in the same manner as for non-parametric electron-beam microwave amplifiers, such as traveling wave tubes^[28,64,65]. The problem of reducing the noise figure is solved in this case using some method of cooling the slow transverse wave of the beam, for example by broadening the beam in a magnetic field to reduce the cyclotron-wave noise and to obtain a beam noise temperature much lower than the cathode temperature^[66,67]. Another method is parametric cooling, which will be considered in the next section.

In conclusion let us note some problems connected with the construction of guns for EPA^[68,69]. To obtain a low noise figure, the noise temperature of the electron beam at the given output should be as low as possible. Depending on the gun construction, this

*The field inhomogeneity in the input capacitor (due, for example, to the edge effects) also leads to an undesirable coupling with the synchronous waves^[45,56].

Table II. Strong coupling between waves in the pumping space.

N _z	$\omega_p > \omega$		$\omega_p < \omega$		$\omega_p \approx \omega$		Amplification condition	Optimal condition	Character of coupling	Change with z
	Coupled modes	Fre- quencies	Coupled modes	Fre- quencies	Coupled modes	Fre- quencies				
1	f.c. f.c.	ω $\omega_p - \omega$	f.c.	ω	s.c.	ω	$ \omega_{pe} - 2\omega_c < 2 \frac{\Omega^2}{\omega_c}$	$ \omega_{pe} - 2\omega_c = 0$	Active	exp.
	s.c. s.c.	ω $\omega_p - \omega$	s.c.	$\omega - \omega_p$	f.c.	$\omega + \omega_p$				
3	f.s. f.s.	ω $\omega_p - \omega$	s.s.	ω	f.s.	ω	$\omega_{pe} < 2 \frac{\Omega^2}{\omega_c}$	$\omega_{pe} = 0$	Active	exp.
	s.s. s.s.	ω $\omega_p - \omega$	f.s.	$\omega - \omega_p$	s.s.	$\omega + \omega_p$				
5	f.c. s.s.	ω $\omega_p - \omega$	f.c. f.s.	ω $\omega - \omega_p$				$\omega_{pe} = \omega_c$	Passive	sin
6	s.c. f.s.	ω $\omega_p - \omega$	s.c. s.s.	ω $\omega - \omega_p$	f.c. f.s.	ω $\omega + \omega_p$		$\omega_{pe} = -\omega_c$	Passive	sin

(f.c. - fast cyclotron, s.c. - slow cyclotron, f.s. - fast synchronous, s.s. - slow synchronous.)

temperature can be either lower or considerably higher than the cathode temperature. It also follows from the foregoing that it is desirable to have a well-focused beam with high space-charge density. To obtain a wide band and small values of F it is also necessary to have high beam perveance and to maintain the longitudinal velocities constant over the beam cross section. The electron rotation frequencies must not fall in the region of internal amplification of the quadrupole. The construction of such guns is a complicated problem. Good results were obtained with six-anode, Brillouin, and immersion type guns^[68]. The beam perveance in these guns is $\sim 3 \times 10^{-6} \text{ A/V}^{3/2}$ at a beam potential $\sim 6 \text{ V}$, a beam current $\sim 40 \mu\text{A}$, and a beam diameter $\sim 0.4 \text{ mm}$. It must be noted that a gun which shapes a beam with low electron temperature reduces both the fast and the slow cyclotron waves to an equal degree.

6. GENERALIZATION OF THE PRINCIPLE OF PARAMETRIC AMPLIFICATION

Starting from the diagrams of Fig. 7 and from conditions (3.12) and (3.13), we can investigate different cases of strong coupling of the modes in a manner similar to that in Sec. 3. The results of such an investigation are listed in Table II^[70]. We see from the table that active parametric coupling is possible not only between two cyclotron waves, but also between two synchronous waves. Only passive coupling is possible between one cyclotron wave and one synchronous wave. We note that pumping at frequencies $\omega_p > \omega$ is called high-frequency, while at frequencies

$\omega_p < \omega$ it is called low-frequency. In accordance with the kinetic-power theorem, amplifiers with low-frequency pumping are not low-noise.

With the aid of the table we explain a method of removing noise from the slow wave, called the parametric cooling method and first proposed by Sturrock^[71]. Parametric cooling is based on the use of passive coupling between a slow wave with negative kinetic power and a fast wave with positive kinetic power. The necessary condition in this case is high-frequency pumping: $\omega_p > \omega$. Thus, to remove the noise of a slow cyclotron wave at a frequency ω we can use passive coupling with a fast synchronous wave at frequency $(\omega_p - \omega)$; the pump unit must satisfy the condition $\omega_{pe} = -\omega_c$ (column 6). The noise of the fast synchronous wave at frequency $(\omega_p - \omega)$ must be first removed by causing the beam to interact with the slow-wave system (a capacitive cavity cannot be used because the synchronous waves have no transverse velocity). If we select the quadrupole length L such that

$$\frac{\Omega^2}{\omega_c u_0} L = \frac{\pi}{2}, \quad (6.1)$$

then complete energy exchange will take place at this length between any pair of passively coupled waves^[36]. The noise of the slow wave goes over into the fast one, and is then removed with the aid of the passive slow-wave system.

We can analogously eliminate the slow synchronous wave at frequency ω , using its coupling with the fast cyclotron wave at frequency $(\omega_p - \omega)$; the pump unit must satisfy the condition $\omega_{pe} = \omega_c$ (column 5). The fast cyclotron wave must first be cooled in a capaci-

tive cavity. Parametric cooling can be used either to produce low-noise amplifiers at the slow mode, or to broaden the region of low-noise operation in the $\omega > \omega_p$ band.

In addition to quadrupole structures such as in Fig. 6, we note a few other electric pump field configurations that ensure coupling between different transverse waves of the electron beam.

a) Twisted quadrupole with rotating pump field [36].

Such a field can be produced by an octufilar helix such as in Fig. 16a. The figure indicates the law governing the variation of the potentials of the individual wires; the plus sign is chosen in the case when the helix is twisted in the same direction as the electrons, and the minus sign in the opposite direction.

The potential in the region of passage of the beam is

$$U_p = \frac{1}{a^2} V_{pm} [(x^2 - y^2) \cos(\omega_p t - \beta_p z) \pm 2xy \sin(\omega_p t - \beta_p z)]. \quad (6.2)$$

The pump field can also be electrostatic ($\omega_p = 0$).

An analysis of the equations of motion in such a quadrupole leads to a diagram that is reminiscent of Fig. 7, but half of the couplings on the diagram will be missing, since the rotating pump field couples only waves with identical polarization [71a].

b) Twisted quadrupole [37, 72]. If the plates of the quadrupole of Fig. 6a have a twist with a constant β_q , the field of such a twisted quadrupole is

$$U_p = \frac{V_{pm}}{a^2} [(x^2 - y^2) \cos 2\beta_q z + 2xy \sin 2\beta_q z] \cos \omega_p t. \quad (6.3)$$

Usually a quadrifilar helix is used in lieu of plates of hyperbolic shape, as shown in Fig. 16b [37]. The pump field can be either alternating ($\omega_p \neq 0$) or electrostatic ($\omega_p = 0$). An analysis of the equations of motion leads to results similar to those of Sec. 3, except that β_p is replaced by $2\beta_q$.

c) Axially-symmetrical pump field. Such a field can be produced by a periodic electric field of the form

$$E_{pz} = E_{pm} \sin(\omega_p t - \beta_p z). \quad (6.4)$$

In accordance with Maxwell's equations, the field varying along z generates a transverse electric field in a direction away from the system axis. The periodic electric field ensures a whole series of interesting parametric couplings between the transverse waves of the beam, including active coupling if $\omega_{pe} = \pm \omega_c$ [36]. An axially-symmetrical electrostatic field can be used in ESA in which the pump structure is in the form of a series of rings (Sec. 7). An investigation of the coupling of different transverse waves in an axially symmetrical field is desirable also when account is taken of lens effects, which can appear in the amplifiers (guns) and can influence their noise characteristics [37, 47].

d) Pumping with two-dimensional fields [36]. In two-dimensional fields (Fig. 16c), the intensity of the transverse field is approximately proportional to the distance from the axis, making it possible to use

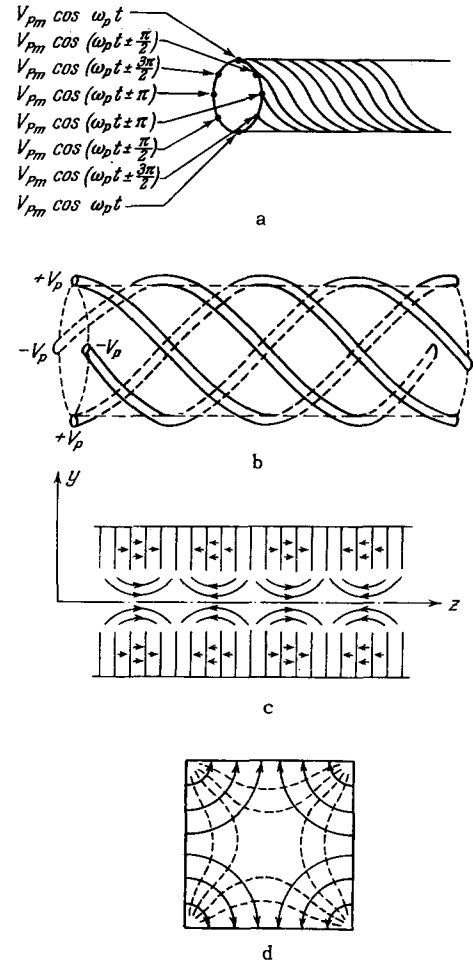


FIG. 16. Types of pump fields. a) Twisted quadrupole with rotating field; b) twisted quadrupole in the form of a quadrifilar helix; c) two-dimensional field; d) field of a TE_{11} wave in a rectangular waveguide.

them in EPA. From the equation of motion it follows that in a two-dimensional field each wave is coupled with all the others. By suitably coupling the waves we can obtain amplification or periodic exchange of power. Two-dimensional fields are simplest to construct, but they give a lower gain.

e) Waveguide structures [26]. A near-quadrupole field configuration exists when a TE_{11} wave propagates in a rectangular waveguide (Fig. 16d) or a TE_{21} wave in a round waveguide. It is also possible to use the two-dimensional field produced when a TE_{20} wave propagates in a rectangular waveguide.

f) Double pump wave. Barnes [73] considered theoretically pumping with the aid of two waves with frequencies ω_{p1} and ω_{p2} , with propagation constants β_{p1} and β_{p2} . The beam formed in this case is rich in harmonics, so that such a device can in principle be used as a harmonic generator. The constructional difficulties in double pumping can be partially overcome by choosing $\omega_{p1} = \omega_{p2}$ or $\omega_{p1} = 0$ and $\omega_{p2} \neq 0$.

In the general case we can consider the motion of the electron beam in an arbitrary electromagnetic pump field. In order for such a field to be physically realizable, it must satisfy Maxwell's equations. The pump parameters in the equation of motion of a beam of the type (3.9) depend in this case on the intensity of both the electric and magnetic fields. A theoretical analysis of the coupling between the transverse waves in a linearized electromagnetic pump field of arbitrary form makes it possible to obtain all the known cases of strong interaction^[74]. As follows from the analysis, the arbitrary electric field can be replaced in principle by a corresponding magnetic field, which results in a similar interaction of the transverse waves.* Amplifiers and harmonic generators (frequency converters) with magnetic, especially magnetostatic, pumping are also feasible.

The conditions for strong coupling in the pump region can be written in the form^[74-76]

$$\omega_{pe} \approx \tau \omega_c, \quad \tau = 0, \pm 1, \pm 2, \quad (6.5)$$

with $\tau = -2, -1, 0$ corresponding to the plus sign in (6.2), and $\tau = 2, 1, 0$ —to the minus sign. The approximate equality in (6.5) indicates that a strong interaction exists in some vicinity of these frequencies. Optimal coupling is realized at the exact equality. Active coupling is possible between two cyclotron waves when $\tau = \pm 2$, between two synchronous waves when $\tau = 0$, and passive coupling is possible between one cyclotron and one synchronous wave when $\tau = \pm 1$. It is interesting to note that $|\tau|$ coincides with the number of cyclotron waves that participate in the given coupling^[75]. The synchronism conditions (6.5) for a Doppler pump frequency ω_{pe} can also be obtained graphically by considering the rotation of electrons in coupled waves^[75].

It is possible to investigate similarly an input (output) coupler unit of the general type with an electromagnetic field^[77]. An investigation shows that there is no difference in principle between couplers with electric or magnetic fields, and only some mixed coefficients play any significant role. It is possible to realize different combinations ranging from purely electric to purely magnetic fields. The kinetic-power theorem holds true in the coupler of the most general type. Couplers are possible not only for cyclotron but also for synchronous waves^[77, 78, 78a], based on the passive coupling between the fast synchronous wave and the forward wave of the system (line). An investigation of the operation of the input coupler yields many interesting results concerning the energy exchange between transverse waves, the

*In theory it is possible to have not only amplifiers but also generators operating at the transverse beam modes. In this case energy flows not from the pump structure into the electron beam, but vice versa. The operation of the device is based, of course, on the use of the slow wave, that is, on the deceleration of the electron beam^[74].

scatter of longitudinal velocities, the role of harmonics, etc.^[77].

7. TYPES OF AMPLIFIERS

a) Adler amplifier. The degenerate amplifier of the Adler type is presently the most advanced of all electron-beam parametric amplifiers. In Table III are listed results obtained with several EPA of this type^[4]. The column headings indicate the published source of the data. In the table δ_0 is the beam diameter, f_s the signal frequency, f_p the pump frequency, P_p the pump power, D the dynamic range, etc. In the construction of the amplifier it is necessary to solve many complicated technological problems, which, nonetheless, can be overcome.* Figure 17 shows a photograph of one of the EPA described in^[57], while Fig. 18 shows the dependence of its noise figure F on the frequency. A whole series of other EPA is under development, in particular metal-ceramic tubes of increased rigidity with external tuning of the operating frequency band^[81], and also various commercial models^[82, 83a].

EPA were tested in radars, in navigation devices,

Table III. Characteristics of electron-beam parametric amplifiers

Literature	31	57	79	80
$I_0, \mu A$	35	27	40	78
U_0, V	6	40	6	21
δ_0, mm	0,44	0,38	1,04	0,4
B_0, G	200	1470	72	420
f_s, Mcs	560	4137	200	1175
I_p, Mcs	1120	8274	400	2340
P_p, mW	10	150	2	150
G, dB	20-30	19	10	20
$\Delta f, Mcs$	50	32	25	55
F, dB	0,9-1,4	0,79	1,6	1,6
$T_n, ^\circ K$	30-70	25±10	80	55
D, dB		100	80	

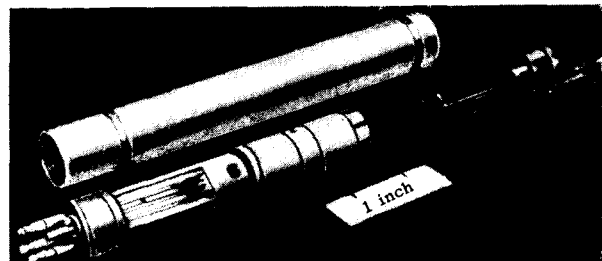


FIG. 17. Experimental electron-beam parametric amplifier.

*One of the requirements imposed on the amplifier is, for example, strict identity of the pump field in all the quadrants. Since, however, hh' and gg' in Fig. 5 are zero equipotentials, it is possible to replace them with metal, so that only one-quarter of the quadrupole remains. The beam then travels eccentrically, but this is of no importance, since the gain does not depend on the beam position. Such a quadrupole is easier to construct^[45].

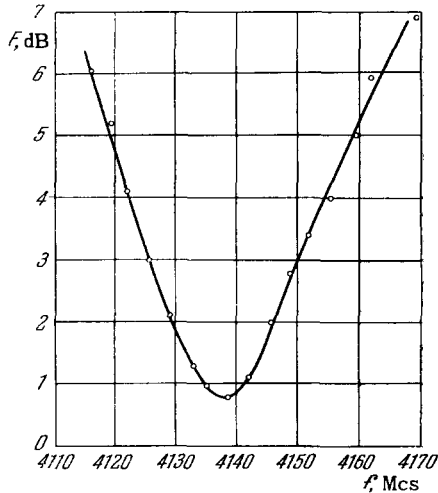


FIG. 18. Dependence of the amplifier noise figure F on the frequency.

in radio astronomy, in systems for radiosonde observation and for satellite observations, and elsewhere [81,84-86]. A considerable reduction in noise was attained, from 8-18 dB (prior to the use of the EPA) to 1.4-3.4 dB. The level of the minimum discernible signal increased by 3-15 dBm (when operating with the pump frequency in the passband). The scanning range of radar and navigation equipment was increased 70% through the use of EPA operating in the passband, and 45% when operating outside the passband.

Radioastronomy signals are broad-band, and therefore the presence in an idler frequency broadens the band of the instrument. A large input signal to the EPA only causes the beam to settle on the plates of the quadrupole or of the output resonator, but produces no damage. This makes it possible to protect the succeeding parts of the installation. The recovery time following an overload is fractions of a millisecond. A valuable property of EPA is the high phase and amplitude stability, and also the stability of the gain during operation. The service life of EPA is higher than that of other electron-beam amplifiers, since its cathode operates at low voltage and current. Interesting experiments were made in the use of EPA in receiving systems with phase synchronization [82]. There are prospects of reducing the noise figure to its two-channel value in this case.

b) Nondegenerate EPA [34,87]. In this amplifier (Fig. 19) the electron beam passes through two couplers in succession. The first is an ordinary capacitive cavity in which the signal is introduced and the beam noise at frequency $\omega_s = \omega_c$ is removed. The second device is used to remove the beam noise at the idler frequency $\omega_i = |\omega_s - \omega_p|$ and constitutes a parallel plate capacitor, twisted in accordance with the instantaneous shape of the beam excited in a

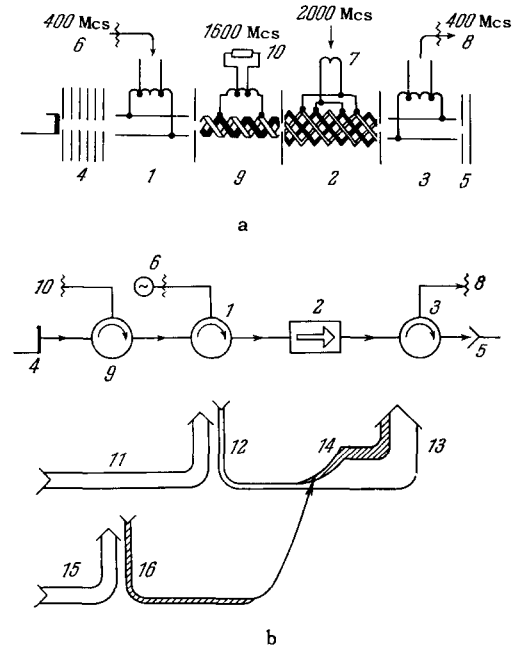


FIG. 19. Equivalent circuit (a) and operating principle (b) of a nondegenerate EPA. 1 - Input unit at signal frequency; 2 - amplification region; 3 - output unit at signal frequency; 4 - gun; 5 - collector; 6 - signal input; 7 - pump input; 8 - output of amplified signal (load); 9 - output unit for idler frequency; 10 - load of idler frequency; 11 - noise of beam at signal frequency; 12 - noise of idler source; 13 - amplified signal noise; 14 - idler load noise, transformed to the signal frequency; 15 - beam noise at idler frequency; 16 - load noise at idler frequency.

fast cyclotron mode with frequency ω_i . * This is followed by a twisted quadrupole in the form of a quadrifilar helix and an output cavity similar to the first cavity.

Figure 20 shows the ω - β diagram of the experimental amplifier. To reduce the noise figure, it is desirable to choose $\omega_s \ll \omega_i$. According to the Manley-Rowe relation, the residual noise of the beam is distributed among the modes (in the quadrupole) in proportion to their frequencies, and the signal wave is partially rid of noise. In an experimental tube $f_s = 400$ Mc/s, $f_i = 1600$ Mc/s, and $f_p = 2000$ Mc/s. The quadrupole constant is $\beta_p = \beta_i$, since $\beta_s = 0$. The noise figure F is 1.9 dB, of which 0.4 dB is due to the losses in the input unit. This, however, is the single-channel, that is, the practically-realizable noise figure. Of the remaining 1.5 dB or 120° K, 75° K represents thermal noise in the idler frequency

*If the noise at the idler frequency is not eliminated, it makes a contribution equal to $T_k \omega_s / \omega_c$ to the noise temperature, regardless of the value of ω_i . Indeed, the noise temperature of the idler wave at the output from the gun [58] is $T_i = T_k \omega_i / \omega_c$, where ω_c is the cyclotron frequency at the cathode. Substituting T_i in (5.1), we obtain [58] $F = 1 + (\omega_s T_k / \omega_c T_0)$. Therefore cooling of the idler wave is essential.

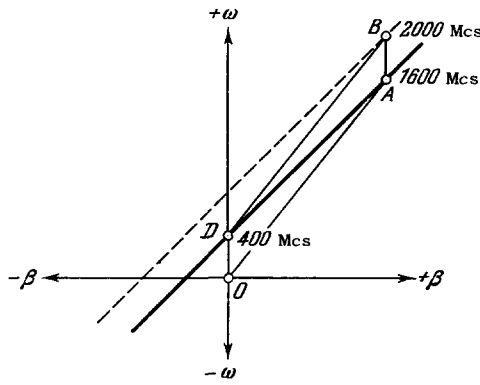


FIG. 20. ω - β diagram of nondegenerate EPA.

channel (one-quarter of the 300° K given by the Manley-Rowe relation, or 75° K goes over into the signal-frequency channel), 20° K the residual noise at the signal frequency, and 25° K the influence of the scatter of the longitudinal velocities of the frequency ω_i , for which $\beta_i \neq 0$. When the coupler for the idler frequency is cooled with liquid nitrogen, it is possible to obtain $F = 1.3$ dB.

c) Amplifier with low-frequency pumping [88,89].

The use of such equipment can be advantageous in those cases when it is desirable to reduce the pump frequency, for example, when going over to millimeter wavelengths. Particularly interesting are amplifiers that have an ordinary quadrupole with straight plates (Fig. 6a) and capacitive input couplers. The equation describing the interaction between the beam and the pumping field is a Mathieu equation. The regions in which growing solutions exist are located in the case of a Mathieu equation near the values

$$\omega_p = \frac{2}{n} \omega_s \quad (n = 1, 2, 3, \dots). \quad (7.1)$$

A gain $G \approx 10$ dB was obtained in an experimental tube [88] with $n = 3$ and $f_s \approx 300$ Mc/s. To obtain this gain it is necessary to have an appreciable pump amplitude (the gain G is proportional to Ω^6/ω_c^6). The amplifier has many other shortcomings which make its practical utilization difficult.

d) Electrostatic amplifiers (ESA). There are several modifications of ESA. The Gordon amplifier [90,91], the amplifier with sectionalized quadrupole (Fig. 21) [92,93], the amplifier with twisted quadrupole [37], and the amplifier with two-dimensional pumping [94] employ the active coupling between fast and slow cyclotron waves. The amplifier with axially-symmetrical electrostatic field produced by a system

of rings employs active coupling between cyclotron and synchronous waves with oppositely directed power flux and polarization [95]. To reduce the noise figure of an ESA it is possible to use, besides the methods described in Secs. 5 and 6, also a noise transformer near the cathode, at the discontinuities of the longitudinal magnetic or longitudinal electric field [96]. It is advantageous to reduce the diameter of the cathode or to go over to ribbon-type electron beams. If the different methods are used correctly, it is possible to obtain at the output of the gun a beam noise temperature considerably lower than the cathode temperature (according to certain theoretical estimates [96], down to 140° K). It is suggested that eventually, taking into account the absence of the idler wave, the ESA will be able to compete in noise figure with the Adler amplifier [96].

Calculations show that in the regime where the collector potential is depressed, the ESA amplifier can operate with high efficiency, reaching 25–35% [97]. At high efficiencies, a noticeable slowing down of the electron beam takes place, and the pitch of the quadrupole must accordingly be reduced in order to maintain synchronism [93]. The ESA may prove to be a promising instrument for use in millimeter waves.

e) Amplifiers for synchronous waves were investigated theoretically [75] and experimentally [98,98a].

Amplifiers are possible with high-frequency and low-frequency pumping, particularly electrostatic. One experimental tube employed active coupling between a slow (fast) synchronous wave at frequency ω and a fast (slow) synchronous wave at frequency $\omega - \omega_p$ ($\omega + \omega_p$) with $\omega_{pe} = 0$.

f) Type M amplifiers. In the type M electron parametric amplifier [99,100] the magnetic field is directed perpendicular to the constant beam velocity u_0 . The introduction of the signal, the removal of the noise, and the amplification can occur either in different sections (Fig. 22a) or in the same section (Fig. 22b). The electrons execute cycloidal motion in crossed electric and magnetic fields. Some experimental results are described in [99].

Operation of an amplifier with a backward wave is possible. A type M amplifier with electrostatic field was also described [101].

g) Frequency converters and multipliers. An electron parametric amplifier, like any other parametric device, is always a frequency converter, owing to the presence of the idler frequency $\omega_i = |\omega - \omega_p|$. The transformation coefficient can be

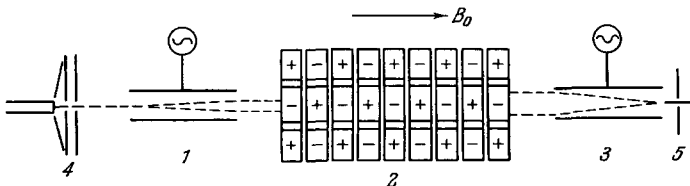


FIG. 21. Electrostatic amplifier with sectionalized quadrupole. 1 – Input coupler; 2 – electrostatic quadrupole; 3 – output coupling unit; 4 – gun; 5 – collector.

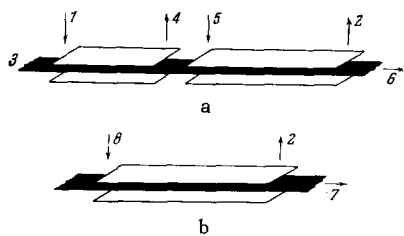


FIG. 22. Type M amplifier. 1 – Signal input; 2 – signal output; 3 – gun; 4 – noise power output; 5 – pump output; 6 – collector; 7 – beam noise power output to collector; 8 – signal and pump input.

determined from the Manley-Rowe relations. In many cases harmonics can also be generated at frequencies $\omega + n\omega_p$, where $|n| > 1$ [74].

Multipole structures can be used as frequency multipliers [33,34]. Figure 23a shows an octupole structure, in which frequency doubling was produced with up to 33% conversion efficiency [45]. There was no pumping, and the field in the octupole was produced by a strong input signal of several mW power. It is possible to replace the octupole by a simpler structure, shown in Fig. 23b. In the structures of Fig. 23 it is possible to obtain also harmonics of higher order, for example the fourth. The possibility of effective frequency multiplication in an electrostatic multipole was investigated theoretically [102]. The beam excitation is specified in this case in the form of two synchronous waves. In an electrostatic $2n$ -pole, the frequencies produced are $(n \pm 1)\omega$, $(2n \pm 1)\omega$, etc., and as the beam moves it assumes the form of an n -blade propeller, the shape of which is rich in harmonics.

h) Pumping with a magnetic field. Amplifiers with magnetic-field pumping were considered only theoretically [74,103,103a]. In particular, an investigation was made of magnetostatic amplifiers, which have different configuration of the transverse magnetostatic field [104,104a], and of amplifiers with discontinuities in the longitudinal magnetic field [105]. In the latter case the magnetic field, that is, ω_c , can reverse sign at the discontinuity. Reversal of the sign of ω_c is equivalent to a reversal of the sign of the

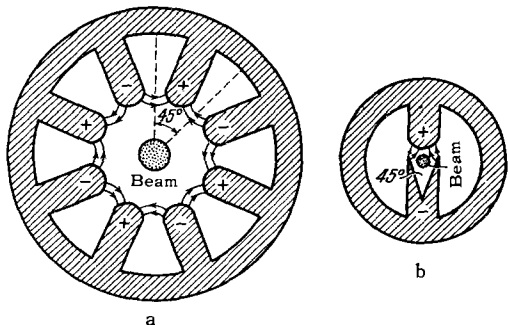


FIG. 23. Octupole structure (a) and its equivalent structure with eccentric beam (b).

kinetic power (2.8), that is, to interchange of fast and slow waves of the beam. To produce a magnetic pump field, one can use permanent magnets or magnetic screens (rings, etc.) made of high permeability material. A coupled-mode analysis of such amplifiers [74,104a] does not lead to any qualitatively new results compared with other types of EPA.

i) Magnetless amplifiers. Amplifiers in which there is no magnetic field are also possible. Electron rotation is produced in such amplifiers by a corresponding electric-field configuration in the input (output) coupler and in the amplification region. Thus, an electrostatic input unit for coupling with the fast cyclotron wave, in the form of a cylindrical capacitor with transverse field, is described in [106,107]. In [108] is described a magnetless electrostatic amplifier with a system of lenses shaping the electron beam. The absence of a magnetic field eliminates the condition $\omega_s = \omega_c$, which is present, for example, in the Adler amplifier, and facilitates the transition to high frequencies. However, the practical suitability of such instruments calls for further study.

CONCLUSION

The electron-beam paramagnetic amplifier with transverse field (EPA) is a new type of electronic device, with many interesting properties.

Such devices have very low noise figures and an appreciable bandwidth. Their sensitivity exceeds that of the better types of traveling wave tubes; EPA have many advantages over parametric semiconductor amplifiers in that they have operating stability, can withstand microwave overloads, and circuits with EPA have no need for cumbersome circulators, since the electron-beam tube itself provides total decoupling in the channel. Electron parametric amplifiers offer many promising applications. They are used as input stages in receivers for very weak signals. They are particularly useful in astronomy, where the noise figure is determined by its two-channel value.

Electrostatic parametric amplifiers (ESA) can be used as amplifiers for small and medium power. In principle, they can also be used as low-noise input amplifiers.

The physical picture of the processes in electron parametric amplifiers is very interesting and rather complicated. Many papers are therefore devoted to the physical properties of EPA, to the interaction of cyclotron and synchronous waves, to the use of various methods of pumping, and to ways of decreasing the noise figure. The physical processes dealing with the interaction of the signal and noise waves with the pumping wave are well described by the coupled-mode theory.

Further improvement in electron beam paramagnetic amplifiers with transverse field should follow the path of broadening of the frequency band of the

operation of the instrument, reducing the working wavelength, and further reduction in the noise figure.

It is convenient to base the theory of transverse-field amplifiers on the matrix method, which is closely connected with the coupled-mode method. Coupled modes make it possible to interpret the physical picture of the processes both in the input units of the electron parametric amplifiers, and in the pump space.

A study of the physical processes makes possible many recommendations concerning the decrease in the noise figure of amplifiers. The theory is essentially in satisfactory agreement with experiment.

¹ T. Lauret, *Toute la radio*, 235, 269 (1959).

² G. Wade, *PIRE* 49, 880 (1961).

³ H. Klinger, *Elektr. Rundschau* 16, 341 (1962).

⁴ M. Kenmoku and T. Matsuoka, *J. Inst. Electr. Commun. Engrs. Japan* 46, 462 (1963).

⁵ *Foundations of Future Electronics*, Ed. by L. D. Langmuir and W. D. Herschberger, N. Y.—Toronto—London, McGraw-Hill, 1961.

⁶ E. Gordon, *BSTJ* 39, 1603 (1960).

⁷ S. Shigebumi, *PIRE* 49, 969 (1961).

⁸ S. Shigebumi, *J. Inst. Electr. Commun. Engrs. Japan* 44, 1749 (1961).

⁹ J. Pierce, *J. Appl. Phys.* 25, 179 (1954).

¹⁰ J. Pierce, *BSTJ* 33, 1343 (1954).

¹¹ W. Louisell, *Coupled Mode and Parametric Electronics*, Wiley, N. Y., 1963.

¹² M. Pease, *J. Appl. Phys.* 31, 1988 (1960).

¹³ M. Pease, *J. Appl. Phys.* 31, 2028 (1960).

¹⁴ M. Pease, *PIRE* 49, 488 (1961).

¹⁵ M. Pease, *J. Appl. Phys.* 32, 1145 (1961).

¹⁶ M. Pease, *J. Appl. Phys.* 32, 1736 (1961).

¹⁷ M. Pease, *J. Appl. Phys.* 33, 2398 (1962).

¹⁸ E. A. Coddington and N. Levinson, *Theory of Ordinary Differential Equations*, McGraw Hill, 1955.

¹⁹ D. K. Faddeev and V. N. Faddeeva, *Vychislitel'nyye metody lineĭnoĭ algebrы (Computational Methods of Linear Algebra)*, Fizmatgiz, 1960.

²⁰ E. Chu, *IRE PGED Electron Tubes Research Conference*, Durham, New Hampshire, June 1951.

²¹ W. Louisell and J. Pierce, *PIRE* 43, 425 (1955).

²² H. Haus and D. Bobroff, *J. Appl. Phys.* 28, 694 (1957).

²³ V. M. Lopukhin, *Radiotekhnika i ělektronika* 6, 683 (1961).

²⁴ A. Siegman, *J. Appl. Phys.* 31, 17 (1960).

²⁵ E. Gordon and A. Ashkin, *J. Appl. Phys.* 32, 1135 (1961).

²⁶ C. Johnson, *J. Appl. Phys.* 31, 338 (1960).

²⁷ Y. Matsuo and A. Sasaki, *J. Inst. Electr. Commun. Engrs. Japan* 45, 1056 (1962).

²⁸ *Noise in Electronic Devices*, ed. by L. D. Smullin and H. A. Haus (Russ. Transl.) "Energiya" Press, 1964.

²⁹ R. Adler, *PIRE* 46, 1300 (1958); also *Radiotekhnika i ělektronika za rubezhom* 1, 88 (1959).

³⁰ Adler, Hrbek, and Wade, *PIRE* 46, 1756 (1958).

³¹ Adler, Hrbek, and Wade, *PIRE* 47, 1713 (1959).

³² C. Cuccia, *RCA Rev.* 10, 270 (1949).

³³ C. Cuccia, *RCA Rev.* 21, 228 (1960).

³⁴ W. Beam, *Rec. Intern. Congress on Microwave Tubes (Munich, 1960)*, *Nachrichtentechn. Fachber.* 22, 362 (1961).

³⁵ H. Tuffil and M. Wharmby, *J. Electronics Control* 11, 47 (1961).

³⁶ R. Gould and C. Johnson, *J. Appl. Phys.* 32, 248 (1961).

³⁷ A. Siegman, *PIRE* 48, 1750 (1960).

³⁸ P. Tien, *J. Appl. Phys.* 29, 1347 (1958).

³⁹ C. Barnes, *PIRE* 52, 64 (1964).

⁴⁰ J. Manley and H. Rowe, *PIRE* 44, 904 (1956).

⁴¹ E. I. Vasil'ev and V. M. Lopukhin, *Radiotekhnika i ělektronika* 9, 1087 (1964).

⁴² H. Tuffil and A. Williams, *J. Electronics Control* 11, 401 (1961).

⁴³ G. Chalk, *Proc. IEE* B110, 2105 (1963).

^{43a} V. Dubrovec, *Arch. Elektr. Übertragung* 18, 585 (1964).

⁴⁴ A. I. Tolpeko, *Trudy, Kiev Polytech. Inst.* 45, 43 (1963).

⁴⁵ A. Ashkin, *Rec. Intern. Congress on Microwave Tubes (Munich, 1960)*, *Nachrichtentechn. Fachber.* 22, 364 (1961).

⁴⁶ T. Bridges et al., *ibid.* p. 352.

⁴⁷ R. Kompfner, *ibid.* p. 403.

⁴⁸ C. Lea-Wilson, *PIRE* 48, 255 (1960).

⁴⁹ M. M. Kovalevskiĭ and A. S. Roshal', *Izv. VUZov, Radiofizika*, 6, 1195 (1963).

⁵⁰ P. Hart and C. Weber, *Rec. Intern. Congress on Microwave Tubes (Munich, 1960)*, *Nachrichtentechn. Fachber.* 22, 358 (1961).

⁵¹ N. Chakraborty, *J. Electron. Control* 10, 147 (1961).

⁵² R. Kompfner, *J. Brit. IRE* 10, 283 (1955).

⁵³ H. Johnson, *PIRE* 43, 874 (1955).

⁵⁴ A. S. Roshal' and V. S. Popov, *Izv. VUZov, Radiofizika* 7, 903 (1964).

⁵⁵ N. Chang, *PIRE* 49, 637 (1961).

⁵⁶ T. Bridges and A. Ashkin, *PIRE* 48, 361 (1960).

⁵⁷ A. Ashkin, *PIRE* 49, 1016 (1961).

⁵⁸ R. Adler and G. Wade, *PIRE* 49, 802 (1961).

⁵⁹ K. Blötekjaer, *J. Appl. Phys.* 33, 2409 (1962).

⁶⁰ T. Wessel-Berg and K. Blötekjaer, *PIRE* 49, 516 (1961).

⁶¹ T. Everhart, *Rec. Intern. Congress on Microwave Tubes (Munich, 1960)*, *Nachrichtentechn. Fachber.* 22, 350 (1961).

⁶² R. Adler et al., *J. Appl. Phys.* 32, 672 (1961).

⁶³ E. Gordon, *PIRE* 49, 1208 (1961).

⁶⁴ H. Haus and F. Robinson, *PIRE* 43, 981 (1955).

⁶⁵ H. Haus and R. Adler, *PIRE* 46, 1517 (1958).

- ⁶⁶ R. Adler and G. Wade, Rec. Intern. Congress on Microwave Tubes (Munich, 1960), Nachrichtentechn. Fachber. 22, 409 (1961).
- ⁶⁷ C. Lea-Wilson et al., J. Electron. Control 10, 261 (1961).
- ⁶⁸ P. Hart and C. Weber, Philips Res. Repts 16, 376 (1961).
- ⁶⁹ P. Hart, PIRE 50, 227 (1962).
- ⁷⁰ R. Krönert, Hochfreq. und Elektroakust. 71, 211 (1962).
- ⁷¹ P. Sturrock, Rec. Intern. Congress on Microwave Tubes (Munich, 1960), Nachrichtentechn. Fachber. 22, 406 (1961).
- ^{71a} R. Fredricks, IRE Trans. ED-8, 212 (1961).
- ⁷² S. Shigebumi and M. Kenmoku, J. Inst. Electr. Commun. Engrs. Japan 44, 916 (1961).
- ⁷³ C. Barnes, IEEE Trans. ED-10, 80 (1963).
- ⁷⁴ K. Blötekjaer and T. Wessel-Berg, Rec. Intern. Congress on Microwave Tubes (Munich, 1960), Nachrichtentechn. Fachber. 22, 372 (1961).
- ⁷⁵ K. Kakizaki, PIRE 50, 2500 (1962).
- ⁷⁶ K. Kakizaki and M. Otomoto, J. Inst. Electr. Commun. Engrs. Japan 44, 1464 (1961).
- ⁷⁷ T. Wessel-Berg, J. Electronics Control 14, 137 (1963).
- ⁷⁸ K. Kakizaki, J. Inst. Electr. Commun. Engrs. Japan 45, 628 (1962).
- ^{78a} C. Johnson, IRE Trans. ED-9, 288 (1962).
- ⁷⁹ G. Chalk, Proc. IEE B108, 125 (1961).
- ⁸⁰ Shigebumi, Masamichi, and Tooru, J. Inst. Electr. Commun. Engrs. Japan 44, 1849 (1961).
- ⁸¹ W. Van Slyck, Proc. Nat. Electron. Conf., Chicago, Ill., Oct. 1961 17, 481 (1961).
- ⁸² Electronics 20, 92 (1960).
- ⁸³ J. Electronics Control 11, 148 (1961).
- ^{83a} Electron Inds. 11, 140 (1961);
- ⁸⁴ R. Adler and W. Van Slyck, IRE Trans. MIL-5, 66 (1961).
- ⁸⁵ Greene, White, and Adler, PIRE 49, 804 (1961).
- ⁸⁶ M. Scanlan et al., PIRE 50, 332 (1962).
- ⁸⁷ R. Adler and C. Hrbek, IEEE Trans. ED-10, 1 (1963).
- ⁸⁸ J. Carrol, Rec. Intern. Congress on Microwave Tubes (Munich, 1960), Nachrichtentechn. Fachber. 22, 356 (1961).
- ⁸⁹ J. Carrol, J. Electronics Control 11, 321 (1961).
- ⁹⁰ E. Gordon, Rec. Intern. Congress on Microwave Tubes (Munich, 1960), Nachrichtentechn. Fachber. 22, 389 (1961).
- ⁹¹ E. Gordon, PIRE 48, 1158 (1960).
- ⁹² J. Bass, Rec. Intern. Congress on Microwave Tubes (Munich, 1960), Nachrichtentechn. Fachber. 22, 382 (1961).
- ⁹³ J. Bass and M. Wilson, J. Electron. Control 11, 125 (1961).
- ⁹⁴ J. Bass, PIRE 49, 1957 (1961).
- ⁹⁵ J. Bass, PIRE 49, 1424 (1961).
- ⁹⁶ T. Wessel-Berg and K. Blötekjaer, IRE Trans. ED-9, 388 (1962).
- ⁹⁷ H. Curnow, J. Electronics Control 11, 161 (1961).
- ⁹⁸ J. Lucken, PIRE 51, 1233 (1963).
- ^{98a} R. Hayes, IEEE Trans. ED-11, 98 (1964).
- ⁹⁹ J. Klüver, Rec. Intern. Congress on Microwave Tubes (Munich, 1960), Nachrichtentechn. Fachber. 22, 367 (1961).
- ¹⁰⁰ J. Klüver, J. Appl. Phys. 32, 1111 (1961).
- ¹⁰¹ W. Sackinger, PIRE 51, 1059 (1963).
- ¹⁰² J. Berghammer et al., AEÜ 17, 345 (1963).
- ¹⁰³ P. Robson, PIRE 49, 645 (1961).
- ^{103a} K. Blötekjaer, IRE Trans. ED-9, 27 (1962).
- ¹⁰⁴ T. Wessel-Berg and K. Blötekjaer, PIRE 50, 2513 (1962).
- ^{104a} K. Blötekjaer and B. Malsness, J. Electron. Control. 14, 187 (1963).
- ¹⁰⁵ H. Seunik, AEÜ 17, 113 (1963).
- ¹⁰⁶ R. Pantell, Rec. Intern. Congress on Microwave Tubes (Munich, 1960), Nachrichtentechn. Fachber. 22, 385 (1961).
- ¹⁰⁷ R. Pantell, IRE Trans. ED-8, 39 (1961).
- ¹⁰⁸ W. Veith, Rec. Intern. Congress on Microwave Tubes (Munich, 1960), Nachrichtentechn. Fachber. 22, 369 (1961).

Translated by J. G. Adashko